

Responses to comments from Referee #1

Thank you very much for your comments and suggestions. Providing this valuable feedback has helped to improve the current manuscript. We have modified the manuscript, taking into account all referee's suggestions. The following contains our detailed responses to your comments, with our responses in plain type given underneath your original comments in bold type.

The manuscript is very well written and understandable. It shows a sensitivity analysis of the multi radar Doppler variational vertical wind velocity retrieval technique based on a simulated convective event as a function of the number of radar involved and their position, radar scan strategy and time sampling. Although most of the technical aspects are described by words or using citations, perhaps the Authors could evaluate to describe some parts in more formal details e.g. by adding appendix for example to describe the coupling of WRF outputs and electromagnetic simulations of backscattering cross section used in the manuscript. I recommend for publication after some minor revisions.

Thank you for the referee for the appreciation. The radar simulator software and its user's guide are publicly available at <https://you.stonybrook.edu/radar/research/radar-simulators/>. The user's guide includes detailed descriptions about how the WRF output is coupled in the simulator and what electromagnetic scattering assumption is used. We would like to skip repeating the descriptions in the manuscript. Moreover, we are preparing to publish a separate paper to introduce the simulator and its applications.

Here we briefly describe about how the WRF output is coupled and the scattering assumption for the referee's reference.

The CR-SIM forward simulator is tailored to compute radar observables by integrating scattering properties over particle size distributions (PSDs) for each hydrometeor, on the basis of microphysics schemes incorporated in the weather model simulation. The environmental variables are obtained from the WRF model output variables and/or calculated using the obtained variables if necessary. Scattering properties of single particles are calculated using the T-matrix method and packaged as look-up tables (LUTs) in the simulator. The simulated 'idealized' observation variables are provided at each gridbox of the input model grid.

The LUTs compose the computed complex scattering amplitudes for equally spaced particle sizes using a T-matrix method developed by Mishchenko and Travis (1998) and Mishchenko (2000). The LUTs for each hydrometeor class corresponding to the model simulation data (e.g., liquid cloud, rain, snow, cloud, ice, graupel) are pre-built by setting particle phase, particle bulk density, and particle aspect ratio. For each hydrometeor class, the complex scattering amplitudes are pre-calculated for the total of 91 elevation angles from 0° to 90° with a spacing of 1°, different temperature ranges for liquid hydrometeors, different possibilities of particles densities for solid hydrometeors, and few different assumptions about particle aspect ratios.

Discussion paper

Main comments

1. Reflectivity weighted mean velocity: I am wondering if its calculation depends by the assumption made on the parameterization of the particle size

distribution within the numerical weather model used. For example, if you assume two different WRF run one using a microphysical schemes 1 and a second independent run using a microphysical schemes 2 which is different by the previous scheme and assume that both microphysical schemes are constrained by the same mixing ratios for a given WRF grid point. Would you obtain two different reflectivity weighted mean velocity for the two assumed microphysical schemes? Am I right? Although I understand that within an OSSE scheme is not necessary reproduce the true (unknown) Doppler velocity from WRF outputs for a single radar, I would suggest the Authors to add some comments in this aspect. Is it worth performing a sensitivity test with respect to the particle size distribution assumption to understand if your simulated velocity fields are consistent with what we expect during actual observations?

Parameterizations of the calculation of the reflectivity-weighted mean fall velocity (e.g., particle size distribution and V_f -D relationship) depend on the assumptions in the microphysical scheme used in the WRF simulation. The referee is right; if we use data from different WRF simulation coupled with a different microphysics scheme, the reflectivity-weighted mean fall velocity calculation follows the parameterizations of the microphysics scheme used. Therefore, the calculated reflectivity-weighted mean fall velocity could be different even if the simulated mixing ratio was same.

We agree with the referee that a sensitivity test to see an impact of particle size distribution assumption on the simulated Doppler velocity field is worthwhile. The present study, however, focused on uncertainties attributed to radar observation sampling in the retrieved wind field, rather than in an assessment of uncertainty of observed Doppler velocity due to microphysics by using the forward simulator. We would like to include the sensitivity test to a separate paper where we study impacts of hydrometeor particle assumptions, such as size distribution, terminal velocity, bulk density, and aspect ratio, on the simulated radar variables (reflectivity, Doppler velocity, and polarimetric variables). Thank you for the valuable suggestion.

We have tested a sensitivity of hydrometeor fall speed estimates to the vertical velocity retrieval. Please see a response to the referee #2's second comment.

2 In the advection correction section when you state: "The high temporal resolution WRF output allows us to evaluate the impact of advection and evolution of the cloud field during the time period needed to complete the radar network VCP." I am wondering if the 0.5 km horizontal resolution-WRF you are using resolves the processes involved within a time gap of 20 s or if 20s is just the time sampling used to write out the simulations. Later on when you state on page 15: "...the number of coherent updrafts structures show little sensitivity to the VCP time. This can be attributed to the fact that the number of updraft coherent structures does not change within the 5 min required to complete all sampling strategies". Can it be attributed to the fact that you are not resolving processes at very short time scales although you have an output at such scales?

The WRF simulation was performed with a time step of 2 seconds and output was saved every 20 seconds. We believe that the WRF simulation captured short time evolution well. Since we used outputs every 20 seconds in the analysis, the radar simulator analysis in this study might not capture the dissipation and formation of updraft cores within 20 seconds. Although it is possible that a few of the updraft cores dissipated or formed within 5 minutes, as we can track individual updraft cores using the

20-sec outputs (e.g. Fig. 3), the evolution of updraft cores was captured by the 20-sec outputs, and the number of updraft cores did not change significantly within 5 minutes.

3. It would be probably nice to add a table in the paper that summarize the results quantitatively (e.g. RMS).

We calculated root mean square errors (RMSEs) of UF, MF, and \bar{w} profiles for the updraft thresholds 5 m s⁻¹ and 10 m s⁻¹ profiles above 2 km AGL for all experiments and added Table 3 to present those values in the revised manuscript.

Minor:

- page 5, lines 1-10: items 1-4: I am wondering if the gridding procedure (spherical to Cartesian) is introducing some errors and if the Authors took them into account. Which is the interpolation method used? Is interpolation in step 3 really needed or it is something done for facilitating gradients calculations?

Because we created radar polar coordinate datasets to emulate the radar sampling strategies, the gridding is mandatory before applying the 3DVAR wind retrieval used in this study. We interpolated the created radar polar coordinate data into the Cartesian grid using the Barnes distance-dependent weighting technique (Eq. 1 of the manuscript). But, for the 3FullGrid simulation, the gridding procedure was not applied because we used the original grid.

The referee is correct. The gridding process can also be an error source in the vertical velocity retrieval. This error can be included and seen when we compare the 3FullGrid simulation with the other simulations using radar VCPs. We discussed about this in the second paragraph of Section 3.1 in the revised manuscript. We used fixed settings for the gridding for all radar simulations except 3FullGrid in the manuscript, and therefore the differences between the radar simulation results (except 3FullGrid) may not include uncertainties attributed to the settings for gridding process.

- page 5 line 13 and hereafter: maybe is “equivalent radar reflectivity factor”.

Done. We used a word “equivalent radar reflectivity factor” or “Z” in the revised manuscript.

- Eq. 1. It is not clear if you are applying the weights only in the horizontal plane or not. In other words, I was expecting that polar to Cartesian conversion was applied in 3D and not in 2D as Eq. 1 is suggesting. Please clarify.

We used this equation for both horizontal and vertical interpolations for gridding. We added the following sentence after the equation: “The equation was applied in both horizontal and vertical interpolations.”

Pag 12, line 17, “The corresponding plots for the latest model output (12:19:40 UTC) used to forward simulate the highest elevations of the 2-min VCP are shown in Fig. 3 (middle row).” Middle row of figure 3 shows 12:19:00 and not 12:19:40.

We replaced the plots in the middle row with those at 12:19:40 UTC and revised the last sentence of the Section 2.4.3 to read “The corresponding plots for the 13th model output (4 minutes after the first scan, 12:22:00 UTC) used to forward simulate the highest elevations of the 5-min VCP simulations is shown in Fig. 3 (bottom row).” Moreover, we changed a color scale of the reflectivity plots to clarify convective cores. Thank you for pointing this out.

Pag 12 Advection correction section. What happen when you intercept the bright band in the advection correction scheme?

The advection correction procedure has not been tested in the presence of a bright band. We can only speculate that there is nothing particular about a bright band that would cause special difficulties, because the advection correction technique does not use information that may be difficult to obtain information in bright bands (e.g., the detailed nature of the scatterers or the terminal velocities). If bright bands are horizontally inhomogeneous, the spatial variations should be able to be "tracked" with the advection correction technique as other reflectivity features are tracked. However, if there is a persistent largely homogeneous bright band covering the entire horizontal domain, the bright band might cause some problems.

In the present study, the radar simulator did not consider melting hydrometeors, thus a bright band was not distinguished in the simulated radar reflectivity fields. Therefore the advection correction was not affected by an issue that is caused by a presence of a bright band, if any.

Fig4. May be I would add a third and fourth row of panels showing the differences between the various scenarios and the original one.

We agree with the referee. However, because the horizontal grid box size is different between the WRF data (0.5 km) and the simulated retrieval data (0.25 km), we decided not to include the horizontal cross sections of the difference for the simulated retrieval from the WRF data. Instead, we added RMSEs of the profiles in Table 3 as suggested in the previous comment.

Figure 5. labels a, b,c, d, e are missing. Upper left panel: “2 min” is missing for the dark grey line.

Done.

Responses to comments from Referee #2

Thank you very much for your comments and suggestions. Providing this valuable feedback has helped to improve the current manuscript. We have modified the manuscript, taking into account all referee's suggestions. The following contains our detailed responses to your comments, with our responses in plain type given underneath your original comments in bold type.

General comment

The paper presents a sensitivity study aiming to address the error sources that affect the X-band Doppler radar-based retrieval techniques of vertical air motion. The main added-value of this work just lies in the comprehensive discussion of the limitations of such techniques. The paper productively contributes to add and extend the current research literature on this topic and can be accepted after some minor revisions.

Thank you for the referee's appreciation for the study.

Specific questions/issues

In my opinion, this study has one main limitation that needs to be considered and discussed. Such issue deals with the estimation of hydrometeors fall velocity (V_f). The authors state (Page 9, Lines 16-17) that V_f used in their work is the one predicted by WRF model simulation; therefore, they assume that no errors related to V_f are introduced in their experiment. In a more realistic scenario, the retrieval of wind field from radar Doppler measurements is strongly related to the variability of the terminal fall velocity of hydrometeors, which constitute a great source of uncertainty. I suggest to carry out, if possible, an additional experiment considering a scenario in which the hydrometeor fall speed is estimated from radar reflectivity measurements and not prescribed by WRF model or, at least, a more comprehensive discussion about the relationship between radar-estimated V_f and wind retrieval.

We agree with the referee that the hydrometeor fall velocity estimate can be a source of uncertainty. We have tested an impact of V_f estimate using reflectivity-based mass-fall velocity relationships proposed by Caya (2001) on the retrieved vertical velocity (presented below). The relationships generally tend to produce slower fall speeds than the reflectivity-weighted mean fall velocities calculated for the WRF simulation case. The retrieved vertical velocity areas from the simulation using the relationships were underestimated. For the referee's reference, we show a comparison between the simulated reflectivity-weighted fall velocity and a relationship for liquid from Caya (2001) and a comparison of the updraft fraction (UF) profiles with the WRF simulation and the 3FullGrid simulation using the relationship. However, the result does not necessarily mean that the relationships were incorrect or the retrieval was failure. It is hard to say whether the fall velocity estimate from these relationships or the hydrometeor fall velocity predicted by model simulation is more reliable. The present study focused on the uncertainties attributed to radar observation sampling, and we decided not to include the sensitivity test of the hydrometeor fall velocity estimate.

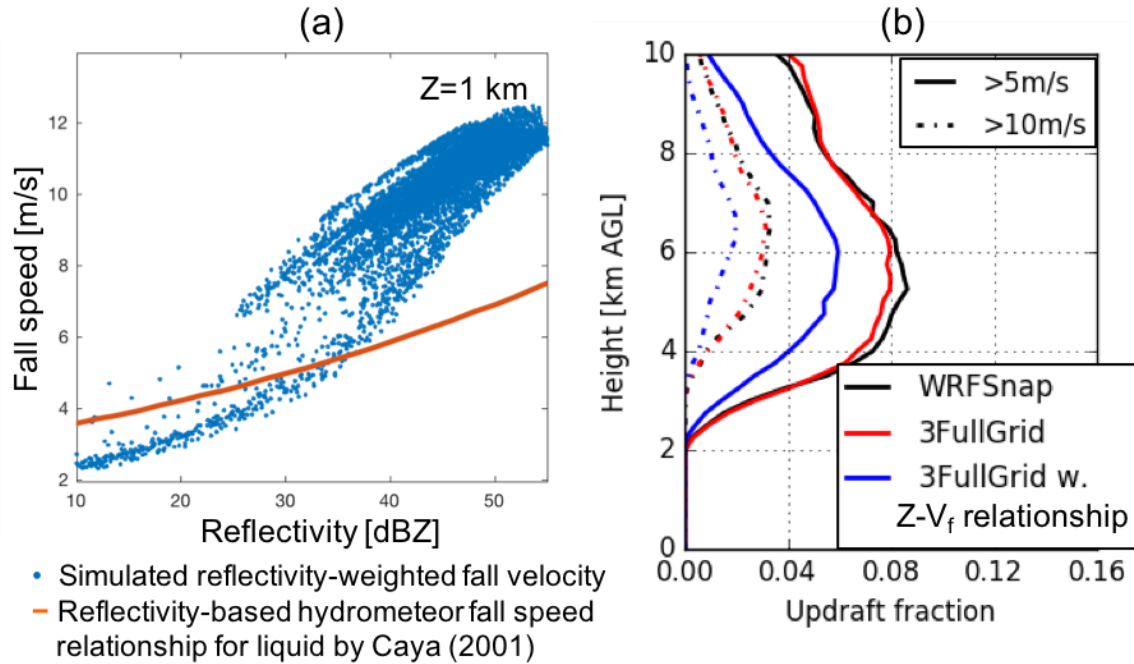


Fig. R1: (a) Simulated reflectivity-weighted V_f versus reflectivity based on the Morrison 2-moment microphysics scheme at a height of 1 km (blue dots) and a reflectivity-based mass-fall velocity relationships for liquid proposed by Caya (2001) (orange line). (b) Vertical profiles of updraft fractions with different thresholds of 5 m s^{-1} (solid lines) and 10 m s^{-1} (dashed lines). In (b), Black lines represent the WRF snapshot at 12:18:00 UTC, red lines represent the 3FullGrid simulation, and blue lines also represents the 3FullGrid simulation, but used the hydrometeor fall velocity estimates proposed by Caya (2001). The reflectivity-based mass-fall velocity relationships for liquid and ice hydrometeors were parameterized:

$$V_f = 5.94M^{0.125} \exp\left(\frac{h}{20}\right) \text{ for liquid}$$

$$V_f = 1.15M^{0.083} \exp\left(\frac{h}{20}\right) \text{ for ice}$$

$$M = \exp\left(\frac{Z - 43.1}{7.6}\right)$$

where h represents height in km, and Z represents reflectivity in a logarithmic scale.

Pag. 9, lines 13-18: the attenuation along the path is one of the main issue affecting the quality of X-band radar measurements. In my opinion, the authors should carry out a more in-depth sensitivity analysis concerning this issue and its possible impact on vertical wind retrieval.

The attenuation for hydrometeors can significantly impact the radar reflectivity measurements, but little impact on the Doppler velocity measurements. However, the attenuation in the reflectivity field can induce underestimations in the reflectivity-based hydrometeor fall velocity estimates. The underestimated hydrometeor fall velocity estimates could induce underestimation of the vertical velocity as shown in the response to the previous comment.

The abstract should be more concise. I suggest to summarize the results in a four or five lines, at most.

We itemized the results in the abstract and reduced the abstract.

Section 2, paragraph 2.1: please add some more details, for the convenience of the reader, about the MCS event considered in this work and about the study area.

We added short descriptions about the observed MCS and WRF-simulated MCS to the first paragraph of Section 2 and Section 2.1, respectively. For the observed MCS, we added: "This squall-line MCS was oriented in northeast-southwest direction extending for approximately 1000 km (Fan et al., 2017). The convective region had approximately 50 km width and trailed a distinct stratiform precipitation area when it passed through the ARM SGP site from 09:20 UTC to 11:40 UTC." For the WRF-simulated MCS, we added: "The simulated MCS comprised a convective precipitation region at the leading edge of the system and a stratiform precipitation trailed by the convective region, as similar as the observation. The MCS passed through the ARM SGP radar observation site approximately one hour later than the observation (at around 12:18 UTC), and a stronger convective precipitation region formed slightly (~20 km) to the north of the ARM SGP site."

Figure 2. Not very clear, in my opinion. Please avoid the use of jet colorbar in panel (c-f).

We changed the color scale for the nearest neighbor distance plots (c-f) in Fig. 2.

The conclusion section should be reduced, by summarizing the main results of the study.

We tried to reduce the amount of the itemized results by removing duplicated sentences.

The results of this study are presented only from a qualitatively perspective. Please introduce some common scores, such as the Root Mean Square Error, that quantitatively summarize the experiments performance.

We calculated root mean square errors (RMSEs) of UF, MF, and \bar{w} profiles for the updraft thresholds 5 m s⁻¹ and 10 m s⁻¹ profiles above 2 km AGL for all experiments and added Table 3 to present those values in the revised manuscript.

Technical corrections

Pag. 2, lines 13 and 20: I suggest the use of the semicolon to improve the sentence structure.

Done. We rephrased the sentence at line 20 as “One drawback of profiling radar techniques is their limited sampling of individual storms and the lack of information on the temporal evolution of the convective dynamics and structure; the observational limitations, thus, make the use of the techniques in model evaluation challenging.”

Pag. 2, line 23: please add “the” before “aforementioned”.

Done.

Pag. 3, line 10 and Pag. 3, line 25: please add a comma before “especially”.

Done.

Pag. 3, lines 11-12: I suggest to revise this sentence.

We revised this sentence to read “Clark et al. (1980) estimated errors attributed to cloud evolution in horizontal and vertical wind estimates from multiple Doppler radar measurements.” Thank you for pointing this out.

Pag. 3, line 13: please add a comma before “by”.

Done.

Pag. 3, line 16: please replace “are” with “have been”.

Done.

Pag. 4, line 8: please add a comma before “that”.

We separated this sentence into the following two: “It is possible that some of the errors are associated with radar volume coverage pattern strategy that does not satisfy the requirement for high spatiotemporal observations.” and “This issue has been highlighted in recent studies with high-resolution CRM simulations of convective cloud properties (e.g., Morrison et al., 2015; Hernández-Deckers and Sherwood, 2016).”

Pag. 4, line 11: please replace “second” with “secondly”.

Done.

Pag. 4, line 16: please add a comma after “to do so”.

Done.

Pag. 4, line 19: please replace “we are investigating” with “we investigate”.

Done.

Pag. 4, line 26: I suggest to use “consists in” instead of “is composed” and to remove “following steps”.

Done.

Pag. 5, line 20: please substitute “retrieved” with “obtained” or “determined”.

Thank you for the suggestion. We used “obtained” instead of “retrieved.”

Pag. 6, lines 3-4: remove “in their study”.

Done.

Pag. 6, lines 5-6: reformulate this sentence.

We rephrase this sentence as “This case has been analyzed for its dynamical and microphysical structures by many previous studies” and moved it to the first paragraph of Section 2.

Pag. 7, line 3: add a comma before “such”.

Done.

Pag. 8, line 5: add a comma before “with”.

Done.

Pag. 8, line 8: add a comma after “box”.

Done.

Pag. 9, line 10: please add “carried out” before “in this study”.

Done.

Pag. 13, lines 10-11: reformulate this sentence.

The advection correction procedure seeks to minimize a cost function that contains the frozen turbulence constraint and terms that confer spatial smoothness on the pattern-translation components. Appropriate values of the coefficient of the spatial smoothness terms depend on the horizontal grid spacing and a typical value of the tracked variable in the case. Based on preliminary tests (not shown), we deemed a coefficient of 300 dBZ^2 to be acceptable.

We added a following phrase to the previous paragraph:

“The advection correction procedure seeks to minimize a cost function that contains the frozen turbulence constraint and terms that confer spatial smoothness on the pattern-translation components.”

and revised the sentence to read:

“A weighting coefficient of the spatial smoothness terms in the cost function coefficient depends on the analysis grid spacing and the structure of the field being advected. An appropriate value of the coefficient can be determined by running some sensitivity tests. Based on preliminary tests (not shown), we deemed a coefficient of 300 dBZ^2 to be acceptable.”

Pag. 13, line 14 and line 15: add a comma after “fields” and before “field”, respectively.

We added a comma after “fields” and “field”, respectively. Thank you for the suggestion.

Pag. 14, line 13: add a comma before “using the original...”.

Done.

Pag. 16, line 18: add a comma before “but”.

Done.

Pag. 16, line 26: please revise “velocities lather than”.

We revised it to read “updraft values.”

Pag. 18, line 14: please remove the comma between “density” and “should”.

Done.

Pag. 21, line 5: please add a comma after “VCP”.

Done.

Pag. 21, line 9: add a comma after "...2016)".

To specify the previous studies, we avoided to add a comma there. Instead, we revised this sentence to read "The rapid evolution of the updraft structures simulated by the WRF are consistent with those from other modelling studies where the temporal evolution of the convective thermals can be significant over time periods larger than 2 min (e.g., Morrison et al., 2015; Hernández-Deckers and Sherwood, 2016)."

Pag. 21, line 27: please replace "were" with "was".

Done. Thank you for pointing this typo out.

Responses to comments from Referee #3

Thank you very much for your comments and suggestions. Providing this valuable feedback has helped to improve the current manuscript. We have modified the manuscript, taking into account all referee's suggestions. The following contains our detailed responses to your comments, with our responses in plain type given underneath your original comments in bold type.

Overarching Comments

This paper describes a rigorous evaluation of the North et al. (2017) 3DVAR multi-Doppler air motion retrieval using a high resolution cloud resolving model and a radar-model simulator and carefully examining selected common sources of uncertainty: characteristics of the scanning strategy, time updates of the scanning strategy, and advection corrections to the data. The novel aspect of the paper is that the experiments can control for many aspects of the sources of uncertainty given the high temporal resolution of the model output which can be subsampled nearly arbitrarily for comparison with the retrievals. The paper makes the case that for some characteristics of estimating vertical velocity in triple-Doppler networks, that having a Doppler radar capable of scanning a PPI in less than 2 minutes is desirable, particularly for accurately estimating the characteristics of weak updrafts.

Thank you for the appreciation for this study.

One major comment I have is that while the paper's methodology is thorough and the figures are clear and illustrative, the presentation of the results is done in an illogical fashion and does not allow for an easy read. The text refers to many multi-panel figures in a repeated fashion that lead the reviewer to do a lot of page flipping. I suggest breaking up the Figures 5, 6, 7, and 8 into different figures that follow the logical flow of Section 3 without having to refer back to the figure subpanels over and over again. Alternatively, discussion of the variables in Figs. 5-8 could be done sequentially by retrieved variable rather than by observing strategy. I believe that the former strategy would be easier for the authors to do.

I believe the paper is acceptable for publication with these minor revisions in mind.

Thank you for the suggestion. We broke Figures 6, 7, and 8 up into three figures:

Figure 6: UF, MF, w profiles for WRF outputs and 3FullGrid.

Figure 7: UF, MF, w profiles for 3XR and 3LR simulations and those for the limited area.

Figure 8: UF, MF, w profiles for 4SR simulations and 3XR simulations coupled with the advection correction.

Specific Comments

1. Should the title be revised to include 3DVAR retrievals? The paper does not include other traditional dual-Doppler retrievals such as in CEDRIC (which have different assumptions about integrating the continuity equation than 3DVAR), or more advanced analyses such as in SAMURAI (Bell et al.). Different techniques could fare better or worse than the 3DVAR technique.

Thank you for the suggestion. We changed the title to “Investigation of observational error sources in multi Doppler radar three-dimensional variational vertical air motion retrievals.” Moreover, we referred to those papers (Miller and Fredrick, 1998 and Bell et al., 2012) in Introduction.

2. It should be stated in the methodology that this analysis is based on a single case, and performance assessment could vary for different storm characteristics and propagation speeds. For example, a slow moving tropical squall line in low vertical wind shear could present less of a challenge for multi-Doppler retrievals than the highly-sheared May 20 MC3E squall line.

Thank you for the valuable comment. We added a following sentence in Section 4: “The assessment of the multi-Doppler radar retrieval presented in this study could vary for different storm characteristics (e.g., isolated storm and less wind shear).”

3. P5, L3, and elsewhere: the apostrophe is unnecessary.

Done.

4. P5, L25: suggest removing the word ‘at’.

Done.

5. P6, L15-16: the CRSIM simulates the phase shift and the differential phase shift, not the phase and specific differential phase, correct?

The CR-SIM can simulate the specific differential phase (K_{DP}) at each gridbox, but not the differential phase shift (ϕ_{DP}).

6. P7, L8: An analysis domain top of 10 km does not top the storm, correct? This would not allow for correct estimation of the storm-top divergence properly in the interpolated simulated radar data. Does this lead to some of the uncertainty unnecessarily?

Correct; the top of the analysis domain (10 km) was not the storm top. Above 10 km altitude, the radar data density more decreases, and an uncertainty in the retrieved vertical velocity can increase with height, because these heights are poorly constrained by radial velocity observation. Collis et al. (2010) showed that radar mapping artifact where radar coverage is poor can lead to minimum vertical velocity errors of the order of 2 m/s at these heights. In our 3DVAR technique, the mass continuity constraint was applied at each grid box, and the calculation was performed until the cost function was minimized without such heights including poor radial velocity constraint. We tested a 3XRSnap simulation including higher altitudes upto 15 km. Figure below shows a comparison of the updraft fraction (UF) profiles with the WRF simulation (black lines) and the original 3XRSnap simulation (red lines). In the present case, updraft fractions for updrafts > 5 m/s and > 10 m/s above 10 km were smaller than 0.04 and 0.005, respectively. The updraft fractions for updrafts > 5 m/s from the new simulation (blue lines) converged

on the small updraft fractions above 10 km, unlike the profile from the original 3XRSnap simulation, However, at other altitudes, errors became larger compared to the original 3XRSnap simulation (e.g., 5-9 km and below 4 km for updrafts > 5 m/s, and 4-8 km for updrafts > 10 m/s). We will need more analysis to address this impact in a separate paper. Thank you for the insight.

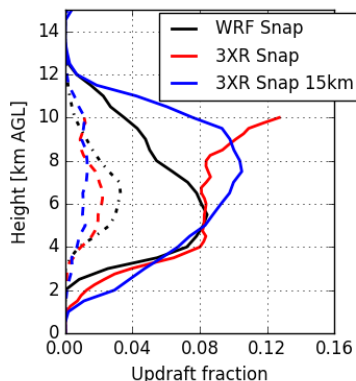


Fig. R2. Vertical profiles of updraft fractions with different thresholds of 5 m s^{-1} (solid lines) and 10 m s^{-1} (dashed lines). Black lines represent the WRF snapshot at 12:18:00 UTC, red lines represent the original 3FullGrid simulation presented in the manuscript, and blue lines represents the 3FullGrid simulation that the vertical domain was extended to 15 km AGL.

7. P8, L20: “not unfolded correctly observed Doppler velocity” needs rewording.

We revised the phrase to read “unfolding of observed Doppler velocity.”

8. P9, L14: “at” should be in.

Done.

9. P13, L2: The tilt would depend on the propagation speed and the vertical wind shear, which in some regimes (especially in the tropics) could be smaller than in this case.

The referee is correct. We revised this sentence to read “horizontal advection and wind shear are expected to tilt the cloud and dynamical structures in vertical.” Thank you for pointing this out.

10. P13, L11: The smoothness function is a Cressman or Barnes filter? If not, what equation did you use?

The advection correction procedure seeks to minimize a cost function that contains the frozen-turbulence constraint and so-called “penalty” terms that confer spatial smoothness on the pattern-translation components. The advection correction procedure is designed to produce smooth pattern-translation components U and V, but does not specifically attempt to smooth the scalar field being advected (i.e., reflectivity in the present study). The smoothness on the U and V components is obtained through the smoothness terms in the cost function, which are proportional to the squares of the horizontal gradients of U and V. As shown in Shapiro et al. (2010), the Euler-Lagrange equations arising

from minimization of this cost function contain terms (arising from the smoothness terms) that involve the Laplacians of U and V. Such terms act to "diffuse" the U and V fields, resulting in smooth U and V solutions. Theoretically, the procedure would preserve spatial discontinuities in the advected scalar field, if discontinuities were present in the input PPI data and if the scalar field satisfied the frozen-turbulence constraint.

For the referee's reference, we would like to show the cost function (Shapiro et al. 2010):

$$J \equiv \iiint \left[\alpha \left(\frac{\partial R}{\partial t} + U \frac{\partial R}{\partial x} + V \frac{\partial R}{\partial y} \right)^2 + \beta |\nabla_h U|^2 + \beta |\nabla_h V|^2 \right] dx dy dt$$

where U and V represent pattern-translation components, and R represents the advected scalar fields, which is the simulated radar reflectivity in the present study. The second and third terms are smoothness terms, and a coefficient β is the smoothness weighting coefficient.

In the revised manuscript, we added a following phrase to the first paragraph of section 2.4.4:

"The advection correction procedure seeks to minimize a cost function that contains the frozen turbulence constraint and terms that confer spatial smoothness on the pattern-translation components."

and revised the sentence to read:

"A weighting coefficient of the spatial smoothness terms in the cost function coefficient depends on the analysis grid spacing and the structure of the field being advected. An appropriate value of the coefficient can be determined by running some sensitivity tests. Based on preliminary tests (not shown), we deemed a coefficient of 300 dBZ² to be acceptable."

11. P14, L1: Suggest inserting "potentially" before "large".

We rephrased this as "large potential uncertainties." In the revised manuscript.

12. P14, L25-26: "...but it tends to have higher uncertainty in the areas around the location of strong convection..." - this seems highly subjective. Can you make a quantitative statement related to this topic?

The updraft fraction for 1-5 m/s from the 3XRSnap simulation was overestimated by 0.1 – 0.17 above 2 km AGL, which accounts for 40-88% of that from the WRF output. The height of the error peak was around 5-6 km, which corresponds to the peak of UF₅ and UF₁₀. We added this description after this sentence.

Discussion paper

13. P15, L7: Regarding an updraft core defined as being larger than 0.5 km²: Is

this at a single level? This is one single pixel, correct? Since the retrieval has a resolution that is effectively 4-6 times the grid spacing, would one expect it to retrieve such small updraft features? Perhaps it is not surprising then that the retrievals have such issues resolving updrafts (particularly weak ones) that are single pixels in the grid? Perhaps increasing this threshold to have larger-sized updrafts (say larger than 2-3 km³) would reveal different uncertainties.

This threshold corresponds to 8 pixels for the wind retrieval data and 2 pixels for the WRF data at a single level. The referee's comment is right; in the retrieval, a single data point could affect surrounding several grid points. Therefore we carefully decided this threshold to remove such noise in the retrieval results.

14. P15, L16: Suggest inserting an "A" before "Noticable".

Done.

15. P16, L8-10: This sentence is awkward.

We rephrased this sentence as "In subsequent sections, a more detail analysis of the impact of the different options in the observational setup on the UF, MF and \bar{w} profiles are discussed."

16. P20, L12-13: "cloud evolution cannot maintain the instantaneous cloud structures": Can you be more specific what you mean by this?

We rephrased this sentence as "cloud evolution alters vertical and horizontal distributions of hydrometeors and vertical velocity, resulting in observing different cloud life stages by different PPI scans."

17. P22, L6: "As previous literature has pointed out..."

Done.

18. P22, L8: 4.5 km is mid-levels, no?

We changed it to "> 4.5 km."

19. P22, L16: Need comma after "i.e."

Done.

20. P22, L18: "inferior" should be "lower"?

The word "inferior" means "lower in quality" in this sentence. We would like to use this word here.

21. P22, L28: Suggest replacing “hard” with “challenging”.

Done.

22. P23, L10: Scott G.’s last name is misspelled.

We are sorry about this. We corrected it in the revised manuscript.

23. P23, L20: “DOW’s” should be “Doppler on Wheels mobile radars”

Done.

Responses to comments from Referee #4

Thank you very much for your comments and suggestions. We have modified the manuscript, taking into account all referee's suggestions. The following contains our detailed responses to your comments, with our responses in plain type given underneath your original comments in bold type.

This paper investigates the impact of some sources of uncertainty on multiple-Doppler analysis of ground based radar data, with emphasis on vertical velocity. It is well written, clear and easily understandable. In fact, I don't have much to say about the points raised by the authors. The analysis process is good and the scientific argumentation is excellent.

Having said that, however, I am a little sceptical about the overall impact of this work and its general interest for the radar user community. Without being rude, it seems quite obvious that improving the VCP, the number of radars, or the time sampling resolution will have a positive impact on retrieved wind fields and, in particular, vertical velocity.

Discussion paper

This has been shown previously by many authors in many different radar network configurations. While I agree that findings and recommendations resulting from this study would be useful for ARM RGP laboratory users, they would be difficult to apply to other networks. Furthermore using numerical model outputs and radar simulators to build a reference wind field is quite common nowadays and cannot be considered as a new concept.

Actually reading section 2.3 of the paper should generate quite some frustration among any scientist interested in radar wind retrieval. Indeed, questions regarding the impact of prescribed hydrometeor fall speed, potential masks, attenuation by rainfall (especially at X-band), or velocity folding count among the main sources of questioning for users and developers of multiple-Doppler analysis methods. To the best of my knowledge, these issues have never really been addressed to date and I was hoping that this study would help to clarify them, which would have contributed to make this paper a truly original contribution to the field. To be consistent with my remark, however, I must mention that the study on the impact of advection is original and does answer important questions.

To sum up, the work presented by the authors is of good quality, but its contribution to the field with respect to previous studies seems quite poor to me and results are barely applicable to networks other than ARM RGP laboratory. From there I see two options: 1/ Improving the paper by investigating additional sources of uncertainty such as V_t , velocity folding, attenuation... among others, or 2/ Clearly state that this study aims to optimize the performance of the ARM RGP network, without seeking to generalize its findings. Option 1 would require substantial additional work, but would undoubtedly represent an important contribution to the field. Option 2 would mostly imply cosmetic work (title, introduction, conclusions), but the impact of this paper would be limited.

Thank you for the referee's appreciation for the study and pertinent comments. As the referee pointed it out, the analysis in this manuscript is limited to a 3DVAR multi Doppler radar technique and impacts of radar sampling limitation. First, we changed the title to "Investigation of observational error sources in multi Doppler radar three-dimensional variational vertical air motion retrievals."

We totally agree with the referee that the hydrometeor velocity estimates and the signal attenuation are major sources of errors in the wind retrieval. We have tested an impact of hydrometeor velocity estimate using reflectivity-based mass-fall velocity relationships proposed by Caya (2001) on the retrieved vertical velocity. Please see a response to the referee #2's second comment. The retrieved

vertical velocities from the simulation using the relationships were underestimated. However, it is hard to say whether the fall velocity estimate from these relationships or the hydrometeor fall velocity predicted by model simulation is more reliable. The present study focused on the uncertainties attributed to radar observation sampling, and we decided not to include the sensitivity test of the hydrometeor fall velocity estimate.

The (along-track) attenuation of hydrometeors can significantly impact the radar reflectivity measurements, but we confirmed that the reflectivity attenuation did not mask the Doppler velocity fields significantly in the analysis area. A figure attached below shows the simulated attenuated and non-attenuated radar reflectivity fields and associated Doppler velocities for the X-SAPR I4 radar at an elevation angle of 4.5 degrees. In all simulations in the present study, we used the Doppler velocity associated with the attenuated reflectivity. On the other hand, the attenuation in the reflectivity field can induce underestimations in the reflectivity-based hydrometeor fall velocity estimates. The underestimated hydrometeor fall velocity estimates could induce underestimation of the vertical velocity as shown in the response to the referee #2's second comment.

Our radar simulator does not include an option of simulating radial velocity folding, and we have not investigated an impact of the folded radial velocity on the vertical velocity retrieval. Recent velocity unfolding techniques can produce unfolded Doppler velocity fields with high accuracy (e.g., James and Houze, 2001). We expect that the folded Doppler velocity issue can be resolved in recent and future studies.

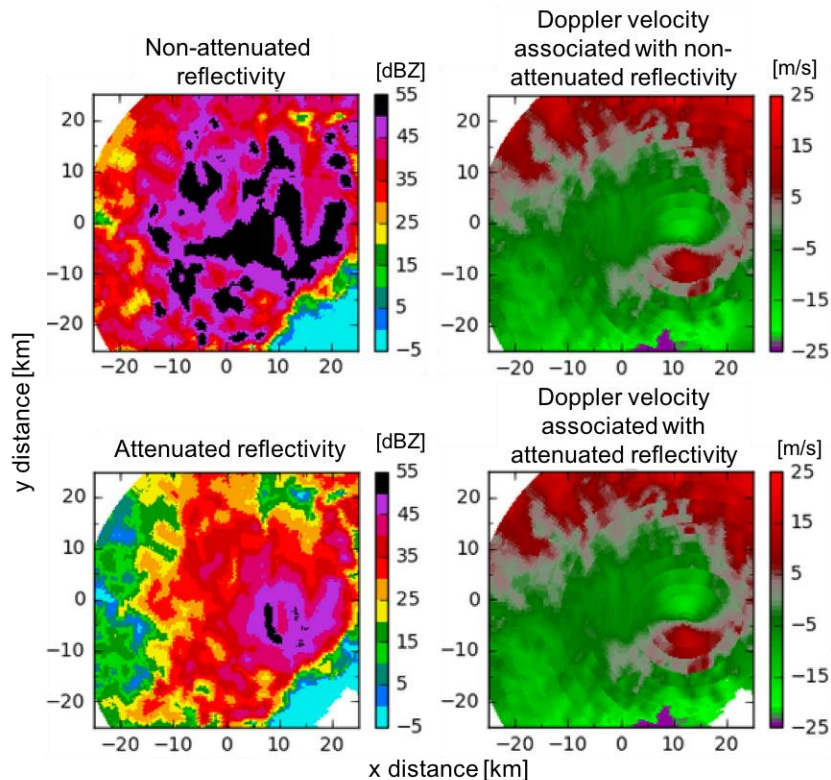


Fig. R3. PPI images of simulated reflectivity without attenuation (top left), Doppler velocity without reflectivity attenuation (top right), reflectivity with along-path two-way attenuation (bottom left), and Doppler velocity associated with the attenuated reflectivity (bottom left) for the X-SAPR I4 radar at an elevation angle of 4.5 degrees at 12:18:00 UTC.

As the referee pointed it out, the results of application of the advection correction to the wind retrieval are consistent with the previous studies; the advection correction is effective for shorter time period VCPs (< 2min). The present study also took into account the volume sampling and compared their impacts. The magnitude of improvement by the increase of elevation angles is larger than that by advection correction, even though the VCP needs 2 minutes. We modified the abstract and conclusion to more simplify them in response to other referee's comments and highlighted the result.

We also agree with the referee that the analysis in this manuscript is limited to the ARM radar network at the Southern Great Plains. Although the manuscript simulated the ARM precipitation radars, the similar radar network has been installed in many regions such as France (e.g., Bousquet et al. 2007), Germany (Helmert et al. 2014), and Japan (Maesaka, et al. 2011), and is expected to be extended to more countries. Moreover, future field campaigns targeting deep convection would be strongly motivated to install multiple Doppler radars to observe vertical air motions in convective clouds (e.g., <https://www.arm.gov/news/features/post/52835>). The present analysis can give valuable information to improve the observation strategies and decide optimized scan strategies for the networks. In the revised manuscript, we added a following sentence to the last paragraph: "Although the present study focused on the ARM X-band radar network, the similar dense radar network has been installed in several regions (e.g., Bousquet et al., 2007; Maesaka, et al. 2011; Helmert et al., 2014) and field campaigns targeting deep convection (past, on-going and future) would be strongly motivated to install multiple Doppler radars to observe vertical air motions in convective clouds. The present analysis can give valuable information to improve the observation strategies and decide optimized scan strategies for the networks."

From a cloud resolving model (CRM) perspective, the present study would notify the CRM communities of large uncertainties in the multi-Doppler radar-retrieved vertical air motion in upper parts of convective clouds, although some of the CRM simulation studies concluded that the CRMs significantly overestimated updrafts compared to multi-Doppler radar vertical velocity retrievals.

We have extended this OSSE study to a tropical convection case from Tropical Warm Pool – International Cloud Experiment and isolated storms over a Houston area. Those OSSEs commonly showed that limited radar sampling would cause underestimation of strong updraft areas. We are preparing separate papers for detailed analyses using the experiments.

References:

- Bousquet, O., Tabary, P., and Parent du Châtelet, J.: On the value of operationally synthesized multiple-Doppler wind fields, *Geophys. Res. Lett.*, 34, L22813, doi:10.1029/2007GL030464, 2007.
- James, C.N. and Houze, R.A.: A Real-Time Four-Dimensional Doppler Dealiasing Scheme. *J. Atmos. Oceanic Technol.*, 18, 1674–1683, [https://doi.org/10.1175/1520-0426\(2001\)018<1674:ARTFDD>2.0.CO;2](https://doi.org/10.1175/1520-0426(2001)018<1674:ARTFDD>2.0.CO;2), 2001.
- Helmert, K., and Coauthors: DWDs new radar network and post-processing algorithm chain. *Proc. Eighth European Conf. on Radar in Meteorology and Hydrology (ERAD 2014)*, Garmisch-Partenkirchen, Germany, DWD and DLR, 4.4, 2014. [Available online at http://www.pa.op.dlr.de/erad2014/programme/ExtendedAbstracts/237_Helmert.pdf]
- Maesaka, T., Maki, M., Iwanami, K., Tsuchiya, S., Kieda, K., and Hoshi, A.: Operational rainfall estimation by X-band MP radar network in MLIT, Japan. *Proc. 35th Int. Conf. on Radar Meteorology*, Pittsburgh,

PA, Amer. Meteor. Soc., 142. 2011. [Available online at <https://ams.confex.com/ams/35Radar/webprogram/Paper191685.html>.]

Other remarks:

1/ Results are based on a single case. Authors should keep that in mind in their conclusions. The effectiveness of vertical wind retrieval depends on many factors, including wind shear for example.

Thank you for the important suggestion. Taking into account the referee #3's suggestion, we added a following sentence to the conclusion: "The assessment of the multi-Doppler radar retrieval presented in this study could vary for different storm characteristics (e.g., isolated storm and less wind shear)."

2/ More details are needed regarding the wind retrieval method used in this paper. What about data interpolation and air-mass continuity equation (e.g., boundary conditions)?

We used the 3DVAR multi-Doppler radar wind retrieval technique shown in North et al. (2017). This technique first needs to interpolate the radar data into the Cartesian coordinate. We used a Barnes distance-dependent weight (Eq. 1 in the revised manuscript) for the interpolation. The equation was applied in both horizontal and vertical interpolations. At each grid box, radar moments are estimated using the nearest 200 radar data gates with weights (Eq. 1) using a smoothing parameter $\kappa = 0.13 \text{ km}^2$ for interpolation. The cutoff distance is determined as the distance where the weight is less than 0.01 ($d \approx 0.8 \text{ km}$). These parameters are chosen so that the statistical error in retrieved vertical velocity is minimal for the present case. These settings for gridding are fixed for all radar simulations. We slightly modified Section 2.3 to briefly describe this gridding method.

As referee #1 pointed out, the gridding process can also be an error source in the vertical velocity retrieval. This error can be included and seen when we compare the 3FullGrid simulation with the other simulations using radar VCPs. We added this discussion to the second paragraph of Section 3.1 in the revised manuscript.

We used the 3DVAR wind retrieval technique described in North et al. (2017). The optimal wind field solution in the technique is obtained at the minimum of a cost function which contains the radial velocity observation constraint, anelastic mass continuity constraint, surface impermeability constraint, background wind field constraint, and spatial smoothness constraint. The mass continuity equation is an element of the cost function, and technique, the constraint was applied at each grid box. We used the surface impermeability constraint to dictate that vertical velocity vanishes at the ground with a relatively large weight. We modified Section 2.3 to read:

"The wind retrieval algorithm inputs the Cartesian coordinate Z and V_r fields from each radar and uses 3DVAR technique continuity constraint proposed by Potvin et al. (2012a). In the technique, the optimal wind field solution in the technique is obtained at the minimum of a cost function which consists of the physical constraints of radar radial velocity observations, anelastic mass continuity, surface impermeability, background wind field, and spatial smoothness. The surface impermeability constraint was used to dictate that vertical velocity vanishes at the ground with a relatively large weight."

3/ More details are needed about the investigated weather system. Authors should include additional material to better describes the overall structure of the storm (e.g. vertical cross-section of model/radar reflectivity/wind fields).

We added short descriptions about the observed MCS and WRF-simulated MCS to the first paragraph of Section 2 and Section 2.1, respectively.

For the observed MCS, we added: “This squall-line MCS was oriented in northeast-southwest direction extending for approximately 1000 km (Fan et al., 2017). The convective region had approximately 50 km width and trailed a distinct stratiform precipitation area when it passed through the ARM SGP site from 09:20 UTC to 11:40 UTC.”

For the WRF-simulated MCS, we added: “The simulated MCS comprised a convective precipitation region at the leading edge of the system and a stratiform precipitation trailed by the convective region, as similar as the observation. The MCS passed through the ARM SGP radar observation site approximately one hour later than the observation (at around 12:18 UTC), and a stronger convective precipitation region formed slightly (~20 km) to the north of the ARM SGP site.”

Moreover, we referred previous studies by Liu et al. (2015), Wu and McFarquhar (2016), and Fan et al. (2017), where dynamical and microphysical structures were analyzed.

Investigation of observational error sources in multi Doppler radar three-dimensional variational vertical air motion retrievals

Mariko Oue¹, Pavlos Kollias^{1,2,3}, Alan Shapiro⁴, Aleksandra Tatarevic³, Toshihisa Matsui⁵

¹School of Marine and Atmospheric Sciences, Stony Brook University, Stony Brook, 11794, USA

5 ²Environmental and Climate Sciences Department, Brookhaven National Laboratory, Upton, 11973, USA

³Department of Atmospheric and Oceanic Sciences, McGill University, Montreal, H3A 0G4, Canada

⁴School of Meteorology, University of Oklahoma, Norman, 73019, USA

⁵ Mesoscale Atmospheric Processes Laboratory NASA Goddard Space Flight Center, Greenbelt, 20771, USA

10 *Correspondence to:* Mariko Oue (mariko.oue@stonybrook.edu)

Abstract. Multi-Doppler radar network observations have been used in different configurations over the last several decades to conduct three-dimensional wind retrievals in mesoscale convective systems. Here, the impacts of the selected radar volume coverage pattern (VCP), the sampling time for the VCP, the number of radars used, and the added value of advection correction on the retrieval of the vertical air motion in the upper part of convective clouds are, examined using the Weather Research and Forecasting (WRF) model simulation, the Cloud Resolving Model Radar SIMulator (CR-SIM), and a three-dimensional variational multi-Doppler radar retrieval technique. Comparisons between the model truth (i.e., WRF kinematic fields) and updraft properties (updraft fraction, updraft magnitude, and mass flux) retrieved from the CR-SIM-generated multi-Doppler radar field are used to investigate these impacts. The findings are: 1) the VCP elevation strategy and sampling time have a significant effect on the retrieved updraft properties above 6 km altitude; 2) 2-min or shorter VCPs have, small impacts on the retrievals, and the errors are comparable to retrievals using a snapshot cloud field; 3) increasing the density of elevations angles in VCP appears to be more effective to reduce the uncertainty than an addition of data from one more radar, if the VCP is performed in 2 minutes; and 4) the use of dense elevation angles combined with an advection correction applied to the 2-min VCPs can effectively improve the updraft retrievals. but for longer VCP sampling periods (5 min) the value of advection correction is challenging. This study highlights several limiting factors in the retrieval of upper-level vertical velocity from multi-Doppler radar networks and suggests that the use of rapid-scan radars can substantially improve the quality of wind retrievals if conducted in a limited spatial domain.

Deleted: : Impacts and possible solutions

Deleted: impact

Deleted: is

Deleted:)

Deleted: In overall,

Deleted: is found to

Deleted: . Retrievals conducted using a

Deleted: show

Deleted: updraft

Deleted: . Increasing

Deleted: and/or

Deleted: can reduce this uncertainty. It is found that the VCP with dense elevation angles appears to be more effective than the addition of data from the fourth radar

Deleted: . The

Deleted: . For

Deleted: errors are considerably larger, and the

Deleted: due to the rapid deformation of the dynamical structure in the simulated mesoscale convective system.

1 Introduction

Measurements of vertical air motion in deep convective clouds are critical for our understanding of the dynamics and microphysics of convective clouds (e.g., Jorgensen and LeMone, 1989). Convective mass flux is responsible for the transport of energy, mass and aerosols in the troposphere, which significantly impact large-scale atmospheric circulation and local environment and affect the probability of subsequent formation of clouds (e.g., Hartmann et al., 1984; Su et al., 2014; Sherwood et al., 2014). Consequently, the vertical air motion estimates are widely employed to improve convective parameterizations in global model (e.g., Donner et al., 2001) and also to evaluate the cloud resolving model (CRM) simulations and large eddy simulations (LES, e.g. Varble et al., 2014; Fan et al., 2017).

Aircraft penetration of convective clouds offer the most direct method to measure the vertical air motions (e.g. Lenschow, 1976); however, practical hazards and operational costs have resulted in a valuable but limited dataset (e.g., Byers and Braham, 1948; LeMone and Zipser, 1980). Current aviation regulation does not permit such penetration anymore. Ground-based and airborne profiling Doppler radars provide a high degree of detail of convective clouds in both time and height and can sample even the most intense convective cores (e.g., Wakasugi et al., 1986; Heymsfield et al., 2010; Williams, 2012; Giangrande et al., 2013; Kumar et al., 2015). One drawback of profiling radar techniques is their limited sampling of individual storms and the lack of information on the temporal evolution of the convective dynamics and structure; the observational limitations, thus, make the use of the techniques in model evaluation challenging.

Since the pioneering work of Lhermitte and Miller (1970), networks of two or more scanning Doppler radars and the use of multi-Doppler radar wind retrieval techniques have been widely used to overcome the aforementioned limitations (Junyent et al., 2010; North et al., 2017). In addition to research radars, operational Doppler radar networks can, in certain conditions, accomplish a large coverage of multi-Doppler radar retrievals (e.g., Bousquet et al., 2007; Dolan and Rutledge, 2007, Park and Lee, 2009). While various Doppler radar wind retrieval techniques have been proposed (Chong and Testud, 1996; Chong and Campos, 1996; Bousquet and Chong, 1998; Gao et al., 1999; Protat and Zawadzki, 1999; Bell et al., 2012), three-dimensional variational (3DVAR) techniques are commonly used because of its robust and reliable solutions by minimizing errors (e.g., Potvin et al., 2012b).

Deleted:),

Deleted: making their

Multi-Doppler radar analysis have been used to better understand mesoscale dynamics, low-level divergence, and microphysical-dynamical interactions (e.g., Kingsmill and House, 1999; Friedrich and Hagen, 2004; Stonitsch and Markowski, 2007; Collis et al., 2013; Oue et al., 2013, and many others). There is also considerable literature discussing different sources of uncertainties in dual- or multi-Doppler radar wind retrieval. The interpolation and smoothing techniques used (Cressman, 1959; Barnes, 1964, Given and Ray, 1994; [Miller and Fredrick, 1998](#)) can have an impact on the quality of Doppler radar wind retrieval (e.g., Collis et al., 2010). Another source of uncertainties is related to the hydrometeor fall speed estimates (e.g., Steiner, 1991; Caya, 2001), especially at shorter wavelengths (e.g., X and C bands) where the signal attenuation can bias the estimates. Clark et al. (1980) [estimated errors attributed to cloud evolution in horizontal and vertical wind estimates from multiple Doppler radar measurements](#). Bousquet et al. (2008) estimated uncertainties in wind fields from their operational multi-Doppler radar retrieval, by simulating radar measurements using numerical model output. They pointed out that missing low-level measurements and poor vertical sampling could produce significant uncertainties in retrieval of low-level wind fields. These investigations [have been](#) conducted by formulating suitable Observing System Simulation Experiments (OSSEs). Potvin et al. (2012b) investigated potential sources of errors in multi-Doppler radar wind retrievals for supercell observations using OSSEs. They suggested that the magnitudes of vorticity and its tendency fields were sensitive to the smoothness constraint in the analysis, and assumptions of spatially constant storm motion and no storm-evolution led to significant errors in middle and upper levels.

A common result from the studies above is that the uncertainties increase with height because scanning radar data density inevitably becomes lower at higher altitudes. Meanwhile, deep convective clouds generally show maximum updrafts at middle and upper parts of the clouds (e.g., Giangrande et al., 2013). Here, we are concerned with the retrieval uncertainties of vertical air motion especially in the middle and upper levels of deep convective clouds. The motivation for this study is two folded. First, the US Department of Energy (DOE) Atmospheric Radiation Measurement (ARM) program operates an atmospheric observatory at Southern Great Plains (SGP), Oklahoma (Mather and Voyles, 2013), where scanning Doppler radars and profiling instruments provide unique dynamical and microphysical measurements. During the Midlatitude Continental Convective Clouds Experiment (MC3E, Jensen et al.,

Deleted:)

Deleted: focused on a difference in spatial scales of convective

Deleted: systems and an impact of

Deleted: sampling volume smaller than model spatial resolution

Deleted: are

2016), the ARM precipitation scanning Doppler radars accomplished dense network of Doppler radar measurements of deep convective clouds explicitly designed to retrieve three-dimensional (3D) wind (North et al., 2017). However, our experience with the data and a series of experiments performed in this study suggest that despite the plethora of radar systems at the ARM SGP observatory, the 3D wind retrievals are subject to large errors especially at the upper levels. It is possible that some of the errors are associated with radar volume coverage pattern strategy that does not satisfy the requirement for high spatiotemporal observations. ~~This issue has~~ been highlighted in recent studies with high-resolution CRM simulations of convective cloud properties (e.g., Morrison et al., 2015; Hernández-Deckers and Sherwood, 2016). ~~Secondly,~~ the paucity of available datasets of vertical air motion limits our ability to quantitatively analyze structures and characteristics of the mesoscale convective systems (MCSs) and evaluate model outputs of the MCSs (e.g., Varble et al., 2014; Liu et al., 2015; Donner et al., 2016; Fan et al., 2017). Thus, we are interested in determining the sampling capabilities required for a multi-Doppler radar network to address these errors and investigating if radar networks based on different technology (e.g., phased-array radars, Otsuka et al., 2016; Kollias et al., 2018a) can address these errors. To do so, we focus on impact of the multi-Doppler radar network setup and not how we quality-control, interpolate or use the Doppler radar observations in a minimization routine. The latter is the same in all the experiments performed here and is described in North et al. (2017). We ~~investigate,~~ the impact of the selected radar volume coverage pattern (VCP), the sampling time for the VCP, the number of radars used and the added value of advection correction upon the uncertainties of multi-Doppler radar wind retrieval.

Deleted: , which have

Deleted: Second

Deleted: are investigating

2 Data and methodology

In this study, the OSSE is conducted for an MCS case on 20 May 2011 observed in Oklahoma during the MC3E. This squall-line MCS was oriented in northeast-southwest direction extending for approximately 1000 km (Fan et al., 2017). The convective region had approximately 50 km width and trailed a distinct stratiform precipitation area when it passed through the ARM SGP site from 09:20 UTC to 11:40 UTC. This case has been analyzed for its dynamical and microphysical structures by several previous studies (e.g., Liu et al., 2015; Wu and McFarquhar, 2016; Fan et al., 2017).

OSSE studies are generally used to assess impacts of operational observing systems on, for example, observation-based value-added products and weather forecasts (Timmermans et al., 2009). The OSSE conducted in this study consists in:

Deleted: is composed of the following steps

- 1) Produce the set of simulation data by a high resolution numerical weather model of a convective cloud system and generate the model hydrometeor and dynamical fields at a high temporal resolution to capture the storm evolution at scales unresolved by typical VCPs;
- 2) Use a sophisticated radar simulator to reproduce the VCP of a multi-Doppler radar system and produce radar observables at radar coordinates with the realistic radar characteristics (beamwidth, range resolution and sensitivity);
- 3) Grid the simulated radar observations to a Cartesian coordinate and conduct a variational 3D multi-Doppler wind retrieval algorithm to estimate the dynamical field; and
- 4) Evaluate the retrieved wind field against the corresponding field from the numerical model direct output.

Deleted: VCP's

The Weather Research Forecasting model (WRF) is used to produce simulation of the MCS case on 20 May 2011 (step 1). The WRF output is used as an input to the Cloud Resolving Model Radar Simulator (CR-SIM; Tatarevic et al., 2018) to simulate equivalent radar reflectivity factor (Z) and Doppler velocity (V_r) from scanning radars (step 2). The simulated Z and V_r fields are then resampled and converted into radar polar coordinate according to VCPs (step 2). The Z and V_r fields at radar polar coordinate are converted into the Cartesian grid, and then they are used to estimate 3D wind field using the 3DVAR multi-Doppler radar wind retrieval algorithm developed by North et al. (2017) (step 3). The obtained vertical velocity fields are compared against the WRF-simulated dynamical field to investigate impacts of the limitations attributed to the radar observations and the retrieval technique on the retrieved vertical wind field (step 4).

Deleted: an

Deleted: observed in Oklahoma during the MC3E

Deleted: radar reflectivity

Deleted: Doppler velocity

Deleted: radar reflectivity

Deleted: Doppler velocity

Deleted: retrieved

2.1 WRF Simulation for 20 May 2011 MCS

The WRF simulation horizontal domain is 960 km x 720 km with 0.5 km horizontal grid spacing. The vertical resolution varies from approximately 30 m near the surface to 260 m at 2 km altitude and maintains this resolution approximately constant above 2 km altitude. To include time evolution in

volume scan coverage pattern, the WRF simulation provides output every 20 seconds. The Morrison double moment microphysics scheme was used, which predicts mass and number mixing ratios for liquid cloud, rain, ice cloud, snow, and a medium density lump graupel representing the rimed ice with a switch to modify the settings for graupel to a high density hail (Morrison et al., 2005). Tao et al. (2016) pointed out that simulations including the hail option better represented the observed MCSs during the MC3E period than those not using hail. In their study for the May 20 MC3E case, Fridlind et al. (2017) used the Morrison double moment microphysics scheme with the hail option. The present study also applies the hail category to the simulation instead of graupel. The simulated MCS comprised a convective precipitation region at the leading edge of the system, and a stratiform precipitation trailed by the convective region, as similar as the observation. The MCS passed through the ARM SGP radar observation site approximately one hour later than the observation (at around 12:18 UTC), and a stronger convective precipitation region formed slightly (~20 km) to the north of the ARM SGP site. In this study, we treat the WRF-simulated vertical velocity field as “truth” to evaluate the performance of multi-Doppler radar wind retrieval.

Deleted: at

Deleted: in their study

Deleted: This case has been actively analyzed for its dynamical

Deleted: microphysical structures (e.g., Liu et al., 2015; Wu

Deleted: McFarquhar, 2016; Fan et al., 2017).

2.2 CR-SIM Simulation of 20 May 2011 MCS case

The CR-SIM is a sophisticated radar forward operator developed to bridge the gap between high-resolution cloud model output and radar observations (Tatarevic et al., 2018). The CR-SIM can be applied on the 3D model output produced by a variety of CRM and LES, such as WRF, Regional Atmospheric Modelling System (RAMS), System for Atmospheric Modelling (SAM), and the ICOSahedral Nonhydrostatic (ICON) model. It emulates the interaction between transmitted polarized radar waves and rotationally symmetric hydrometeors and can simulate the power (equivalent radar reflectivity factor), phase (Doppler velocity) and polarimetric (specific differential phase, differential reflectivity, depolarization) variables with a fixed elevation angle or varying elevation angles with respect to a specified radar location.

Several experiments are performed to evaluate the limitations of the sensing techniques employed in the network of three X-band Scanning ARM Precipitation Radars (X-SAPRs, named I4, I5, and I6, respectively) at the SGP site (Fig. 1), which provided high-resolution radar observations of convective

systems during the MC3E (e.g., North et al 2017). The ARM SGP network is selected because it is comprised by three identical radar systems that are employed together and can be operated in a coordinated manner. Furthermore, since it is a long-term facility for the study of deep convective clouds, it is important to assess the capability and uncertainties. Using CR-SIM, we simulated measurements of the three X-SAPRs. In order to investigate the impact of an increased number of radars, observations from the C-band Scanning ARM Precipitation Radar (C-SAPR) at the SGP site (Fig. 1) are also simulated. Characteristics and settings of the simulated radar measurements are shown in Table 1. To investigate the impact of increasing the number of elevation angles and the maximum elevation angle, a VCP including additional elevation scans for the X-SAPR measurements is introduced. These simulations with X-SAPR aim to examine effects of using faster scanning radars, such as the Doppler on Wheels (DOW, Wurman, 2001), the Atmospheric Imaging Radar (AIR, Isom et al., 2013), the Rapid scanning X-band polarimetric (RaXPoI, Pazmany et al., 2013) and low-power X-band phased array radars (LPAR, Kollias et al., 2018a). Locations of radars used in this study and the simulated retrieval domain are shown in Fig. 1. Details about the elevation angle settings are described in Sect. 2.4.

The retrieval simulation domain size is $50 \text{ km} \times 50 \text{ km} \times 10 \text{ km}$ above the ground level (AGL) centered around the ARM SGP Central Facility (CF). In the simulations, CF and the domain were virtually located within a vigorous convective region of the MCS to capture the intense vertical velocity (Fig 1b). We assume that the lowest boundary of the simulation domain is idealized as flat at the ground level of 0.3 km above sea level.

For each radar, the CR-SIM forward simulated Z_r and V_r are provided at the WRF grid coordinate by CR-SIM. They are then converted into radar polar coordinates considering all the radar characteristics that control the spatial resolution of radar observations (range weighting function, antenna beamwidth, and VCP strategy). The settings shown in Table 1 are consistent with the settings used during the MC3E period. For each radar the minimum detectable signal (Z_{\min}) curve, which is attributed to the number of samples integrated for each radar sampling volume, is estimated using an equation $Z_{\min}(r) = C + 20\log_{10}(r)$. In this equation, Z_{\min} is expressed in logarithmic units (dBZ) with the range r (distance from the radar) in km, and the constant C that depends on the radar system characteristics expressed in dBZ; C

Deleted: reflectivity

Deleted: Doppler velocity

= -40 for X-band radars and $C = -35$ for C-band radar are used in this study. These values are similar to those for X-SAPRs and C-SAPR at the SGP site.

2.3 Wind Retrieval

The 3DVAR wind retrieval technique described in North et al. (2017) is used to estimate the 3D wind field. The wind retrieval algorithm inputs the Cartesian coordinate Z_r and V_r fields from each radar and uses 3DVAR technique continuity constraint proposed by Potvin et al. (2012a). In the technique, the optimal wind field solution in the technique is obtained at the minimum of a cost function, which consists of the physical constraints of radar radial velocity observations, anelastic mass continuity, surface impermeability, background wind field, and spatial smoothness. The surface impermeability constraint was used to dictate that vertical velocity vanishes at the ground with a relatively large weight. Details of the constraints are described in North et al. (2017).

The simulated Z_r and V_r with the radar polar coordinate are converted to the Cartesian coordinates for each radar measurement at horizontal and vertical spacings of 0.25 km using a single-pass isotropic Barnes distance-dependent weight (Barnes, 1964), with a constant smoothing parameter κ .

$$w_{i,q}(d) = \exp\left(\frac{-d^2}{\kappa}\right) \forall i = 1, \dots, n \text{ and } q = 1, \dots, Q \quad (1)$$

Here $w_{i,q}$ is the weight for grid box i and radar gate q separated by distance d . The equation was applied in both horizontal and vertical interpolations. At each grid box, radar moments are estimated using the nearest 200 radar data gates with weights (Eq. 1) using $\kappa = 0.13 \text{ km}^2$ for interpolation. The cutoff distance is determined as the distance where the weight is less than 0.01 ($d \approx 0.8 \text{ km}$). These parameters are chosen so that the statistical error in retrieved vertical velocity is minimal for the present case. Generally, data density at constant altitudes decreases with height and when increasing a distance from radar. Figures 2c-f show distance to the nearest radar data point at each Cartesian grid box at constant altitudes. These settings for gridding are fixed for all radar simulations, and this study does not consider uncertainties attributed to the settings for gridding process. The gridding technique has been well optimized in North et al. (2017), and the uncertainties in the gridding method and data smoothing processes have been well investigated in previous studies (e.g. Majcen et al., 2008; Potvin et al., 2012a).

Deleted: reflectivity

Deleted: Doppler velocity

Deleted: (2012a),

Deleted: capitalizes on

Deleted: radar reflectivity

Deleted: Doppler velocity

Deleted:)

There are several important sources of errors when considering the retrieval of vertical motion in convective systems other than the radar VCP; the most important among them are: unfolding of observed Doppler velocity, estimation of hydrometeor fall velocities, attenuation correction, and assumption of background environments. In all experiments in this study, Doppler velocity folding is disabled as an option, thus, the radial Doppler velocities are unfolded correctly. This eliminates the possibility of errors being introduced by incorrect Doppler velocity unfolding.

The difference between the “true” hydrometeor fall velocity V_f and the assumption based on an empirical formula that relates V_f with the radar reflectivity (e.g., Caya, 2001) can be a possible source of errors in wind retrievals (e.g., Potvin et al., 2012b; North et al., 2017). In the WRF simulations used here, V_f is parameterized depending on the microphysics scheme as a function of particle diameter. The hydrometeor’s fall speeds (V_f) are given as a function of the hydrometeor diameter (D) and altitude (h) in a form:

$$V_f(h, D) = f_c(h) \cdot a_v \cdot D^{b_v} \quad (2)$$

where a_v and b_v are coefficients, and $f_c(h) = (\rho_{surf}/\rho(h))^k$ is the correction factor for air density ($\rho(h)$: air density at height h , ρ_{surf} : surface air density) with exponent k (Morrison et al., 2005; Tatarevic et al., 2018). In the CR-SIM, reflectivity-weighted mean velocity is computed at each grid box in the following manner. The hydrometeor fall speeds as a function of the hydrometeor diameter are averaged over the diameter range with weights that are proportional to the CR-SIM estimated reflectivity for each hydrometeor particle size, and then the mean hydrometeor fall speeds are again averaged over all hydrometeor types present in each grid box with weights of reflectivity. In all experiments carried out in this study, the simulated reflectivity-weighted mean V_f are used in the retrieval, thus, no error attributed to the fall velocity estimates is introduced in the wind retrieval technique.

Another source of errors is the impact of signal attenuation by the hydrometeors along the propagation path, especially in C-band and X-band radar measurements. Since the attenuation is unknown, any attenuation-corrected radar reflectivity acts as a possible error source in the wind retrievals, particularly for hydrometeor fall speed estimates. However, as previously specified, the hydrometeor particle size

Deleted: ,

Deleted: not unfolded correctly

Deleted: at

distributions and V_f used in this study are the ones prescribed by the WRF model microphysics, thus, no error is introduced.

Finally, background horizontal wind vector, temperature, and air density are obtained by averaging WRF output values over the retrieval domain at each altitude and are used in place of sounding measurements over the SGP CF site. Although this study does not consider uncertainties in the background assumption, the change in the background data would have small impact on the retrieved updraft velocities as discussed in North et al. (2017).

2.4 Settings for wind retrieval experiments

Three factors influencing the updraft velocity estimates are investigated. The first is radar volume coverage pattern (VCP) which determines the set of elevation angles used by the radars to sample the volume of the analysis domain. The second is time interval needed by the radars of the network to complete the specified VCP to emulate both the advection and temporal evolution of the convective cloud system. Third, the added value of the advection correction for the different sets of VCP settings is evaluated. The experiments and their names are listed in Table 2.

2.4.1 Control wind retrieval simulation (3FullGrid)

The control wind retrieval simulation is an ideal, instantaneous VCP where all radars of the network sample all the WRF grid points. As a result, three measurements of equivalent radar reflectivity factor and radial Doppler velocity from the three X-SAPRs are available at each grid box of the WRF grid (named 3FullGrid). This experiment does not undergo the conversion process from the WRF grid to radar coordinate or the gridding process from radar coordinate to the Cartesian coordinates. Therefore, this does not include uncertainties from VCP, radar characteristics (beamwidth and range-bin spacing), or gridding process. Thus, the retrieved wind field should be a very good estimate of the true wind field and only the potential uncertainty in the wind retrieval algorithm can affect its quality. In this OSSE, the 3FullGrid is used for an upper bound of the performance of any of the conducted experiments and also serves as a sanity check for the wind retrieval algorithm.

Deleted: or

Deleted:).

2.4.2 Radar VCP

In a typical radar VCP, the number of elevation angles depends on the antenna scan rate and the desired time period for completing the VCP (typically 5-6 min). The antenna scan rate depends on the pedestal technical specifications and the minimum number of radar samples needed to estimate the radar observables with low uncertainty. The elevation angles are generally tightly selected at low elevations to provide good coverage over long horizontal distances and relatively sparse at higher elevations as the X-SAPR's VCP shown in Table 1 and Figure 1c.

In the experiments performed here, the impact of an increased number of elevations angles especially at high elevations is investigated while the antenna beamwidth, range-gate spacing, and maximum unambiguous range are kept unchanged and similar to the radar settings during MC3E. The following VCP are used: i) three X-SAPRs with the general VCP which is the same as during MC3E (named 3XR, Fig. 1c); ii) three X-SAPRs with denser elevation angles (named 3LR, Fig. 1d; the name "LR" stands for low-power X-band phased array radar, LPAR, Kollias et al., 2018a); and iii) same as i) but the C-SAPR measurements are added (named 4SR). Details of the VCPs are shown in Table 1. The settings i) and iii) use general VCPs for X-SAPR and C-SAPR which are the same as those during MC3E. The X-SAPR VCP is composed of 21 elevation angles ranging from 0.5° to 45° , and the C-SAPR VCP is 17 elevation angles ranging from 0.75° to 42° . Elevation angles for the setting ii) are equally distributed from 0.5° to 59.5° with a 1° increment; in total there are 60 elevation angles. This elevation setting intends to simulate rapid scanning radar observations.

The selection of the VCP (XR or LR) affects the density (spacing) and availability of observations at each height for gridding. Figures 2a and 2b show the coverage from the three radars for the retrieval domain for 3XR and 3LR VCPs, respectively. The cone of silence (absence of radar observations) from each radar is represented as yellow circle, in the middle of which the X-SAPR is located. Within the cone of silence of each radar, we only have two available radar measurements for the wind retrieval. In addition to the availability of radar observations, the spacing of the radar observations affect the quality of the gridding. Regions including few radar data points, particularly higher elevation angle regions for the XR VCP, may need to interpolate radar data at longer distances from the grid points. Figures 2c-2f show distance of the nearest radar data point at each grid box at heights of 1 km and 8 km for X-SAPR I6, and

Figs. 2g and 2h show normalized histograms of the nearest distance. At lower altitudes, the nearest distances in the entire retrieval domain (thin lines in Fig. 2h) are mostly less than 0.3 km for both VCPs. At higher altitudes (thin lines Fig. 2h), the distances of the nearest radar data points from the LR VCP are same as at lower altitudes, indicating that the LR VCP has similar radar data density at higher and lower altitudes. For the XR VCP, in contrast, many of grid boxes at 8 km AGL needed to use radar data at distances farther than 0.4 km, resulting in stronger smoothing when the gridding process.

2.4.3 Time duration of the radar VCP

Three time periods are considered here for the completion of the radar network VCP: i) snapshot (named Snap), where it is effectively assumed that the first WRF model output (at time 0 sec, top row, Fig. 3) is frozen in time and the radars instantaneously collect data according as their VCP without any cloud evolution; ii) a 2 minute (named 2min) radar network VCP to emulate the performance of rapid scanning radar networks; and iii) a 5 minute (named 5min) radar network VCP to emulate the performance of the ARM SGP network during MC3E and the performance of other mechanically-scanning radar networks. The 3FullGrid simulation (Sect. 2.4.1) uses a Snap VCP. The Snap VCP eliminates any concerns regarding advection and temporal evolution of the convective cloud and is used as benchmark of performance.

A set of WRF simulations at different times is used to construct the Plan Position Indicator (PPI) scans of the VCP; if a PPI scan takes more than 20 seconds, the WRF output in the following time step is used for the next PPI scan. An example demonstrating how different WRF model outputs are used in this experiment is shown in Fig. 3. Figure 3 shows horizontal cross sections of the Z_r and vertical velocity at 7 km and a vertical cross section of the at the area indicated with the solid line in the horizontal cross sections. The snapshot simulations use the WRF model output data at 12:18:00 UTC (top row). The 2-min VCP simulations use the WRF model output data from six consecutive model outputs extracted from 12:18:00 UTC to 12:19:40 UTC every 20 seconds. Each model output is used to forward simulate 3-4 PPI scans from the C-SAPR and the X-SAPRs, when nominal (MC3E) VCP elevation angles are used (3XR and 4SR) and 10 PPI scans for X-SAPR simulations when the denser elevations angles VCP is simulated (3LR). The corresponding plots for the latest model output (12:19:40 UTC) used to forward

Deleted: radar reflectivity

Deleted: SAPR's

simulate the highest elevations of the 2-min VCP are shown in Fig. 3 (middle row). In accordance, the 5-min VCP simulations use the WRF data for 5 minutes composed of 15 snapshots ranging from 12:18:00 UTC to 12:22:40 UTC every 20 seconds. Each snapshot data was used for 1-2 PPI scans for C-SAPR and X-SAPR simulations with general VCP elevation angles (3XR and 4SR) and 4 PPI scans for denser VCP elevation angles (3LR). The corresponding plots for the 13th model output (4 minutes after the first scan, 12:22:00 UTC) used to forward simulate the highest elevations of the 5-min VCP simulations is shown in Fig. 3 (bottom row).

2.4.4 Advection correction

The high temporal resolution WRF output allows us to evaluate the impact of advection and evolution of the cloud field during the time period needed to complete the radar network VCP. If the cloud field was frozen (no cloud evolution), horizontal advection and wind shear are expected to tilt the cloud and dynamical structures in vertical. Advection schemes have been proposed to address this issue (e.g. Protat and Zawadzki, 1999; Shapiro et al., 2010b; Qiu et al., 2013). The present study used a reflectivity-based spatially-variable advection correction scheme described in Shapiro et al. (2010a) which allows trajectory of individual clouds and smooth grid-box-by-grid-box corrections of cloud locations. The advection correction procedure seeks to minimize a cost function that contains the frozen turbulence constraint and terms that confer spatial smoothness on the pattern-translation components and takes into account changes in cloud shape with time by using two different time PPI scans. The advection correction process is similarly implemented in this case.

The advection correction is applied between two similar elevation angle PPIs from consecutive VCPs. Each simulated Z field in PPI is converted and projected onto the two-dimensional (2D) Cartesian coordinate plane at a spatial resolution of 250 m. A weighting coefficient of the spatial smoothness terms in the cost function coefficient depends on the analysis grid spacing and the structure of the field being advected. An appropriate value of the coefficient can be determined by running some sensitivity tests. Based on preliminary tests (not shown), we deemed a coefficient of 300 dBZ² to be acceptable. Using two 2D Cartesian coordinated PPI data at two different times at the same elevation angle, the advection correction algorithm performs horizontal trajectory analysis of reflectivity and estimates the reflectivity

Deleted: latest

Deleted: 40

Deleted: is

Deleted: as the cloud system moved in a certain direction.

Deleted: This scheme

Deleted: radar reflectivity

Deleted: We used a smoothness

Deleted: 300 dBZ²

Deleted: a

Deleted: in the technique.

pattern translation components U and V on the 2D surfaces for each VCP elevation angle. The pattern translation components U and V fields, along with the associated trajectories of virtual particles moving with the reflectivity field, are then used to effect the advection correction of the radial wind field according to a time difference between a PPI scan and the base PPI scan, when creating the 3D Cartesian coordinated data. Such processed simulated radar measurements in 3D Cartesian coordinates are then incorporated into to the 3DVAR algorithm for the 3D wind retrieval as described in Sect. 2.3.

However, the cloud and dynamical field evolve while advected. This results in observing different cloud life stages by different PPI scans. Figure 3 (right column) shows a vertical cross-section of the vertical air motion within a convective cell that is tracked using the WRF model output. The location of the convective cell and vertical distributions of updrafts and downdrafts significantly vary from 12:18:00 UTC to 12:22:40 UTC. Thus, we need to consider that gridded radar observations collected after the completion of the VCP do not represent an actual snapshot of the 3D convective dynamics. Consequently, the mass continuity constraint will be applied in the column of gridded radar observations that is a mosaic of different stages of the lifetime of a convective element, and this, in turn, will limit the ability for this 3DVAR approach to satisfy the mass continuity equation (e.g., Clark et al., 1980; Gal-Chen, 1982), resulting in large potential uncertainties of the wind retrievals. The experiments presented here are designed to quantify the impact of cloud evolution on the retrieved wind field (Sect. 3.4).

3 Results

The evaluation of multi-Doppler radar-based velocity retrievals using independent observations is challenging to perform (e.g., Collis et al., 2013; North et al., 2017). Profiles of percentiles of updraft magnitudes are often used to evaluate numerical model results against vertical velocity retrievals from scanning Doppler radar networks and/or profiling radars (e.g., Wu et al., 2009; Varble et al., 2014; Fan et al., 2018). Here, we are interested in the estimation of the convective mass flux, thus, profiles of updraft morphology (number and area) and intensity (magnitude) are used to represent the impact of the selected sampling strategy.

3.1 Evaluation of multi-Doppler radar updraft property retrievals

Horizontal cross sections at 7 km AGL and vertical cross sections along $y = 0$ km of the retrieved vertical velocity field from the X-SAPR network, using the original grid (3FullGrid) and using the standard (XR) VCP for three different time periods (Snap, 2min and 5min) are shown in Fig. 4 (b, c, d, and e, respectively). The WRF model out at $t = 0$ (12:18:00 UTC) is also shown in Fig. 4a. The selection of the height of 7 km is based on the WRF model output analysis: the chosen height is the one with maximum updraft values. The WRF model output vertical velocity field indicates the presence of several cell-like, horizontally coherent updraft structures with updraft magnitude exceeding 5 m s^{-1} . The 3FullGrid simulation (Fig. 4b) provides results in good agreement with the original WRF vertical velocity field (Fig. 4a), suggesting that the 3DVAR wind retrieval algorithm is performed well.

The snapshot simulation (3XRSnap, Fig. 4c) provides results that are comparable to the original WRF vertical velocity field and 3FullGrid retrieved vertical velocity field at 7 km AGL, but slightly overestimates the updraft velocity above 8 km AGL (Figs. 4a and 4b). The 3XRSnap simulation reproduces the location and size of the stronger updraft areas defined with updraft magnitudes above 5 m s^{-1} , which show the cell-like structures, but it tends to have higher uncertainty in the areas around the location of strong convection (vertical velocity $< 5 \text{ m s}^{-1}$). Updraft fractions for 1-5 m/s from the 3XRSnap simulation was overestimated by 0.1 – 0.17, which accounts for 40-88% of those from the WRF output. The uncertainty is attributed to the selected radar VCP due to gridding of sparse observations, rather than the 3DVAR wind retrieval algorithm. As increasing VCP time periods (2 min and 5 min) shown in Figs. 4c and 4d, respectively, the retrieved velocity features became less sharp, broader and shifted in space. The retrieved vertical velocity field shows the impact of interpolating the sparse observations (ring structures representing the poor X-SAPR sampling at 7 km) and the vertical velocity features appear elongated and connected.

At any vertical level in the WRF model output and in the retrieved 3D velocity field, a convective updraft core is defined as an area larger than 0.5 km^2 and with updraft velocities higher than 5 m s^{-1} . Figure 5a displays the profiles of the number of updraft cores from the 3FullGrid control wind retrieval simulation and from the WRF snapshot data at 12:18:00 UTC, WRF 2-min average (12:18:00-12:19:40), and WRF 5-min average (12:18:00-12:22:40). As expected, the 3FullGrid retrieved profile of number of

Deleted: XSAPR

Deleted: The uncertainty is attributed to

Deleted: selected radar VCP

Deleted: gridding

updraft cores captures very well the profile of the number of updraft cores in the WRF snapshot model output. Differences appear small between WRF Snap and 3FullGrid and are attributed to the potential uncertainty in the retrieval algorithm. The 2- and 5-min WRF output averaged profiles suggest that the number of convective updraft cores does not change over a period of 2 to 5 min. Figures 5b-e demonstrate performance of the 3DVAR wind retrieval for several different configurations as described in Table 2. A noticeable departure between the WRF direct model output (number of updraft cores) and the estimated number of updraft cores above 6 km AGL is observed for all the detecting configurations with the exemption of the LR VCP. The use of a fourth radar or the implementation of the advection correction has little to no impact on the findings. The retrieved profiles of the number of coherent updrafts structures show little sensitivity to the VCP time. This can be attributed to the fact that the number of updraft coherent structures does not change within the 5 min required to complete all sampling strategies. Another possibility is that any stretching/distortion of the coherent structures due to cloud evolution and advection does not results to changes in the number of coherent structures.

In a similar manner, the retrieved updraft fraction (UF), the retrieved convective mass flux (MF) and the mean updraft velocity (\bar{w}) for the different VCPs are investigated and compared to the direct model output. In this study, convective mass flux (MF) is estimated at each height as:

$$MF = UF \bar{w} \bar{\rho}_d \quad [kg \ s^{-1} \ m^{-2}] \quad (3)$$

where UF is updraft fraction over the domain, \bar{w} is mean vertical velocity over the updraft area, and $\bar{\rho}_d$ is dry air density averaged over the domain. The updraft fraction and mean updraft velocity strongly impact the domain averaged convective mass flux, which can be used to understand mass, energy and aerosol transport by the convective system.

The analysis in this study is presented in Figs. 6, 7, and 8 for the two different updraft thresholds: 5 m s⁻¹ (UF₅, MF₅, \bar{w}_5) and 10 m s⁻¹ (UF₁₀, MF₁₀, \bar{w}_{10}). Furthermore, a comparison limited to a smaller domain where the higher density radar observations are available (squared area in Fig. 2) is added (Figs. 7g-i). Each panel shows their profiles from the WRF snapshot at 12:18:00 by a black solid line (threshold of 5 m s⁻¹) and a black dashed line (threshold of 10 m s⁻¹) for the comparison. Table 3 presents root mean square errors (RMSEs) of UF, MF, and \bar{w} profiles above 2 km AGL for all experiments. In contrast to

Deleted: Noticeable

Deleted: , Fig. 6

Deleted: , Fig. 7

Deleted: , Fig. 8)

Deleted: A

Deleted: 6-8.

Deleted: f). Furthermore, the analysis is presented for the two different updraft thresholds: 5 m s⁻¹ (UF₅) and 10 m s⁻¹ (UF₁₀).

the number of coherent updraft cores, the profiles of UF, MF and \bar{w} exhibit larger sensitivity to the sampling parameters. In subsequent sections, a more detail analysis of the impact of the different options in the observational setup on the UF, MF and \bar{w} profiles are discussed,

Figure 6 compares the WRF snapshot at 12:18:00, the WRF 2-min average, and the WRF 5-min average. The UF profiles from both WRF 2-min average and the WRF 5-min average are in very good agreement with that from WRF snapshot; this consistency is also shown in MF and \bar{w} profiles (Figs. 6b, and 6c, respectively), indicating that the updraft properties are statistically similar throughout the 5 minutes in this case. Figure 6 also compares the profiles from WRF outputs with those from the 3FullGrid simulation. As expected, the UF profiles from 3FullGrid simulation are in very good agreement with the WRF output for all thresholds (Fig. 6a, RMSE < 0.004), but show an underestimation by ~0.01 at 5.3 km AGL. For reference, 1% difference in the updraft fraction corresponds to 25 km² for a 50 km × 50 km retrieval domain. All the retrieved profiles of coherent updraft fraction exhibit considerable differences with the WRF output above 6 km AGL (Figs. 7 and 8). In general, the retrieved updraft fractions increase above 6 km AGL while the WRF output indicates that the updraft fraction decreases.

Figures 6b and 6c show MF and \bar{w} profiles, respectively, from simulated wind retrievals for 3FullGrid together with those from the WRF output. The MF and \bar{w} profiles in the Figures 6b and 6c are coupled with updraft areas for updraft values larger than 10 m s⁻¹ (MF₁₀, \bar{w}_{10}) and for velocities lather than 5 m s⁻¹ (MF₅, \bar{w}_5). For the WRF output, the peaks of MF values are found at heights between 5 and 7 km AGL, and the MF₁₀ values are generally the half of MF₅. The 3FullGrid simulation (Fig. 6b) well captures those features, but the maximum values at 5.25 km AGL are slightly underestimated as MF₅ decreases by up to 0.05 kg s⁻¹ m⁻² (RMSE of 0.02 kg s⁻¹ m⁻²). Since the \bar{w} values are well estimated (RMSE of 0.15 m s⁻¹ for \bar{w}_5), the underestimation is driven by the small underestimation of UF (by 0.01, Fig. 6a).

3.2 Effects of VCP elevation sampling and number of radars

The impact of the maximum elevation angle and density of elevation angles used in the VCP is easily demonstrated when comparing the 3XRSnap and 3LRSnap retrievals for the entire domain (Figs. 7a-f) or within the smaller domain (square area in Fig. 2, Figs. 7g-i). For all updraft parameters investigated here

Deleted: Here, the results are described and

Deleted: are

Deleted: in subsequent sections

Deleted: Figure 6 displays updraft fraction (UF) profiles from different simulations for the two above mentioned updraft thresholds UF₅ and UF₁₀. Each panel shows UF from the WRF snapshot at 12:18:00 by a black solid line for the comparison. Figure 6a also

Deleted: 7a

Deleted: 7b

Deleted:)

Deleted: Fig. 6b, d, e

Deleted: 7

Deleted: 8

Deleted: 7

Deleted: 8

Deleted: velocities

Deleted: 7a

Deleted: .

Deleted: .

Moved down [1]: The mean updraft velocities for both UF₁₀ (\bar{w}_{10}) and UF₅ (\bar{w}_5) from 3LRSnap slightly increase above 6 km AGL (Fig.

Deleted: 8c

Moved down [2]:). Consequently, the MF₅ profile is improved as it increases at 4.5-7 km and decreases above 7 km (Fig.

Deleted: 7c). Similarly, the MF₁₀ profile is also improved as it increases above 4.5 km, but it still underestimated by 0.05 at 5-9 AGL.

Moved down [3]: Compared to the same VCP periods, the 3LRSnap retrievals also show similar improvements at 2-min VCP and 5-min VCP. These results suggest that the VCP with dense elevation angles can improve the retrieval of strong updrafts with velocities larger than 10 m s⁻¹, and is more effective at higher altitudes (> 8 km).

(number of updraft cores, UF, MF, and \bar{w}), the 3LRSnap produces improved comparisons to the direct model output especially when limiting the evaluation area to the center square domain. The comparison for the number of cloud cores (Fig. 5) shows that 3XRSnap overestimated above 6.5 km. Figure 7a shows that UF₅ values from the 3XRSnap are overestimated above 6.5 km AGL, while UF₁₀ values above 6.5 km are underestimated. These profiles indicate that updraft areas of 5-10 m s⁻¹ are overestimated for the 3XRSnap retrievals. Thus, the overestimation of the number of updraft cores is caused by overestimation of updraft areas of 5-10 m s⁻¹. This feature is also shown in other snapshots and 2-min VCP retrievals. The impact of a longer time VCP is more pronounced in the UF retrievals than the number of coherent updrafts cores. As in the case for the profile of the number of coherent updraft cores, the use of the LR VCP improves the updraft fraction profile retrievals.

The UF₁₀ values from the 3XRSnap simulation are underestimated by 0.01 at 5-7 km AGL (~30 % of the true fraction, Fig. 7a) at higher altitudes above 5 km. The errors generally increase with height above 6 km AGL. This result is similar to the dual-Doppler radar wind retrieval OSSE study for supercell storms by Potvin et al. (2012b). The mean updraft velocities are also underestimated by 1 m s⁻¹ for UF₁₀ above 5.5 km (Fig. 7c). The underestimations in \bar{w}_{10} and UF₁₀ profiles result in underestimation of MF₁₀, and the maximum underestimation of 0.1 kg s⁻¹ m⁻² is found at 6 km AGL. For the threshold of 5 m s⁻¹, the overestimation of UF₅ above 7 km results in overestimation of MF₅, while the underestimation of the mean updraft velocity by 2 m s⁻¹ above 4.5 km for UF₅ leads to the underestimation of MF₅ at 4.5-7 km AGL (Fig. 7b).

The mean updraft velocities for both UF₁₀ (\bar{w}_{10}) and UF₅ (\bar{w}_5) from 3LRSnap slightly increase above 6 km AGL (Fig. 7d). Consequently, the MF₅ profile is improved as it increases at 4.5-7 km and decreases above 7 km (Fig. 7e, 24% decrease in RMSE). Similarly, the MF₁₀ profile is also improved as it increases above 4.5 km, but it still underestimated by 0.05 kg s⁻¹ m⁻² at 5-9 km AGL (38% decrease in RMSE). Compared to the same VCP periods, the 3LR retrievals also show similar improvements at 2-min VCP and 5-min VCP. These results suggest that the VCP with dense elevation angles can improve the retrieval of strong updrafts with velocities larger than 10 m s⁻¹, and is more effective at higher altitudes (> 8 km).

Substantially improved retrievals can be obtained in a region near the CF where data density from each radar is higher (square region shown in Fig. 2). Figures 7g, 7h, and 7i show UF, MF, and \bar{w} , respectively,

Deleted: 6b

Deleted: 6b

Deleted: .

Deleted: .

Moved (insertion) [1]

Moved (insertion) [2]

Moved (insertion) [3]

Deleted: 6f, 7f

Deleted: 8f

for the square region. The UF, \bar{w} , and hence MF are improved especially for 3LR simulations, where distances of nearest data are mostly less than 0.2 km (Figs. 2g and 2h). Although the profiles from 3XRSnap and 4SRSnap are improved as they capture the peak at middle altitude, the improvements are weaker than 3LR simulations at higher altitudes, where the distances of the nearest radar data points in the square region are similar as those from the entire domain for XR (Figs. 2g and 2h). It is suggested that the high data density should be considered as an indicator of improved retrievals, as long as the scanning the VCP is completed in 2 minutes.

Increasing the number of Doppler radars in retrievals would reduce the uncertainties as analyzed by Bousquet et al. (2008) and North et al. (2017). Here we compare the 4SRSnap simulation with the 3LRSnap and 3XRSnap simulations (Figs. 8a-c, Table 3). The 4SRSnap retrieval cannot significantly improve the UF₅ and UF₁₀ profiles compared to those from the 3XRSnap, as well as the number of updraft cores and \bar{w} profiles, and hence MF. Lower spatial resolutions of the C-SAPR VCP than the X-SAPR might induce more artifacts in the weaker updraft retrievals. The lower frequency radar (C-SAPR) can provide radar reflectivity measurements that may be easier to correct for hydrometeor and radome attenuation (e.g., Kurri and Huuskonen, 2008). In this case, it is perhaps advantageous to use the lower frequency radar to cover the domain sampled by the XSAPR network. However, if additional radars of the same or better spatial resolution and VCP are available, the network architecture should be considered in order to maximize the triple-Doppler radar area by creating another sampling area with triple-Doppler radar observations.

3.3 Effect of VCP time period

The 2-min and 5-min time period VCP retrievals are compared to the snapshot retrievals to see how the VCP time periods affect the updraft retrievals. For the 3XR retrieval simulations, profiles of the number of updraft cores do not show significant differences among 3XRSnap, 3XR2min, and 3XR5min (Fig. 5b), consistent with little difference among those from WRFSnap, WRF2min, and WRF5min. This feature is also found in the 3LR simulations. However, some differences can be found in Figs. 7a-c, 7d-f, and 8a-c showing updraft fractions, convective mass flux, and mean updraft for 3XR, 3LR, and 3SR simulations. For both updraft threshold of 10 and 5 m s⁻¹, 3XR2min and 3XRSnap UF, \bar{w} , and hence MF

Deleted: .

Deleted: .

Deleted: 6-8

Deleted: .

are in close agreement at all altitudes and even with WRF output (WRFSnap and WRF2min) below 4.5 km, as well as with 3LR and 4SR simulations. The small impacts of 2-min time period are also found for the center square region (Figs. 7g-i). For 3XR5min and 3LR5min simulations, however, UF_{10} , and \bar{w}_{10} are significantly underestimated at 4-9 km AGL (50-110% increase in RMSE for UF_{10} and 40-55% increase in RMSE for \bar{w}_{10} from snapshot simulations) when compared to the snapshot retrievals (3XRSnap and 3LRSnap, respectively). The differences from the 3XR5min simulation result in significant underestimation of MF_{10} at middle altitudes. These differences in UF and MF are also found even when comparing with the WRF UF/MF profiles averaged over 5 minutes (WRF5min). These features are common in 3XR, 3LR, and 4SR simulations. The comparison of UF_5 , \bar{w}_5 , and MF_5 for different time period from a given VCP show different features compared to those for the larger updraft threshold. As discussed in Sect. 3.2, the UF_5 profiles from the simulations are largely overestimated above 6 km and cannot resolve a peak at middle altitudes. The difference becomes larger for the 5-min VCP retrieval simulations. It is suggested that a longer VCP time period tends to underestimate areas of larger updrafts ($> 10 \text{ m s}^{-1}$) and overestimate areas of weaker updraft ($< 10 \text{ m s}^{-1}$). On the other hand, \bar{w}_5 from 3XR5min is underestimated above 5 km. These errors in UF_5 and \bar{w}_5 from 3XR5min produce large underestimation of MF_5 at middle altitudes and overestimation above 7 km. These features are also shown in 3LR5min and 4SR5min, but the underestimations of MF_5 at middle altitudes are small, since underestimation of \bar{w}_5 is relatively small for 3LR5min or overestimation of UF_5 is larger for 4SR5min.

Overall, the impacts from the 2-min VCP on the updraft retrieval can be small, whereas the 5-min VCP can significantly intensify uncertainties especially for stronger updraft regions above 6 km AGL. This is likely due to small convective evolution in 2 minutes while large evolution and advection in 5 minutes as shown in Fig. 3. Potvin et al. (2012b) also showed a similar result that the data sampling in 3 minutes produced significant errors compared to shorter time period (1.5 min) and snapshot for supercell storms. Compared to the 3XR and 4SR retrievals for each VCP time period (2min and 5min), the 3LR2min and 3LR5min show better agreements.

Deleted: 6f, 7f, and 8f

3.4 Effect of Advection Correction

As presented in the previous section, the longer time VCPs more emphasize the uncertainties at upper levels. Because profiles of the updraft properties from WRF output do not change among the snapshot, 2-min average, and 5-min average, the differences found when comparing the simulated retrievals for 2-min and 5-min VCPs without advection correction and those for the snapshot VCPs are probably associated with i) imposed advection and ii) cloud evolution, rather than time change of the updraft properties. Advection will move clouds and cause mismatch of cloud locations between PPI scans from different radars and even from the same radar. Meantime, cloud evolution alters vertical and horizontal distributions of hydrometeors and vertical velocity, resulting in observing different cloud life stages by different PPI scans. Both issues result in deformation of cloud structures and may cause uncertainties in the wind retrieval algorithm, especially the mass continuity assumption is not satisfied adequately. The cloud locations can be corrected using an algorithm proposed by Shapiro et al. (2010a) as described in Sect. 2.4.4. Here, we compare 2-min and 5-min VCP experiments to which the advection correction has been applied (2minadv, 5minadv) with those without the advection correction and snapshot experiments to see how the advection correction can improve the retrievals using 2-min and 5-min VCPs.

Figures 8d-f show UF, MF, and \bar{w} profiles, respectively, from the 2-min and 5-min VCP 3XR simulations corrected for advection (3XR2minadv and 3XR5minadv, respectively), together with those from WRF snapshot and 3XRSnap. The advection-corrected retrievals for the 2-min VCP well improve these profiles as they are closer to the WRF2min profiles and even to the snapshot retrieval (e.g., 16% decrease in RMSE of UF₅ from 3XR2min), while improvements are not significant for the 5-min VCP. Very similar improvements for the 2-min and 5-min VCPs by advection corrections are found in 3LR simulations with advection correction (not shown).

Figure 9 shows comparisons of vertical cross sections between wind retrievals obtained before and after applying the advection correction for the updraft core shown in Fig. 3 (right column). Chosen vertical cross sections go through the maximum updraft area at 7 km AGL. For the 2-min VCP retrievals, regions of updraft values $> 5 \text{ m s}^{-1}$ are significantly corrected by the advection correction technique and maintain the top-left to bottom-right tilt of the WRF updraft structure. It is clear (Fig. 3 right column) that within 5 min the updraft structure has evolved not only in its tilt but also by the presence of a downdraft near its

Deleted: cannot maintain the instantaneous cloud structures

Deleted: observations of

Deleted: 6e, 7e and 8e

Deleted: ,

lower levels. Thus, when using a 5-min VCP, a completely different updraft structure is reconstructed with different tilt and location of the maximum updraft velocity. The difficulty in improving the updraft retrieval using the advection correction, particularly for 5-min VCP, is likely due to fast evolution of convective clouds. The rapid evolution of the updraft structures simulated by the WRF are consistent with those from other modelling studies where the temporal evolution of the convective thermals can be significant over time periods larger than 2 min (e.g., Morrison et al., 2015; Hernández-Deckers and Sherwood, 2016).

4 Summary and conclusions

Convective motions affect microphysical processes and control the transport of moisture, momentum, heat, trace gases and aerosols from the boundary layer to the upper troposphere. Accurate characterization of the convective transport requires vertical air velocity retrievals especially in the middle and upper part of convective cloud systems, and multi-Doppler radar networks have been used to probe convection and provide wind retrievals including vertical air motion estimates. While there is a plethora of studies illustrating the ability of multi-Doppler radar observations to capture the low-level wind divergence and circulation, there is little to show regarding the capability of this observing system to capture the upper level convective dynamics. This study addressed potential observational sources of errors in X-band triple-Doppler radar three-dimensional variational (3DVAR) updraft retrieval using a sophisticated forward radar simulator (CR-SIM) with the WRF simulation output for an MCS on 20 May 2011 during the Midlatitude Continental Convective Clouds Experiment (MC3E) for a domain of 50 km × 50 km × 10 km. An extensive sensitivity analysis is conducted to investigate impacts of radar volume coverage pattern (VCP), the number of radars used for the multi-Doppler radar analysis, time periods for VCP (2 and 5 minutes), and advection correction. An advection correction technique proposed by Shapiro et al. (2010a) was applied to the 2-min and 5-min VCP radar data. Updraft properties such as updraft fraction, mass flux, and updraft magnitude profiles with two different thresholds (5 m s⁻¹ and 10 m s⁻¹), from simulated multi-Doppler radar wind retrievals using three X-band Scanning ARM Precipitation Radars (X-SAPRs) are examined. The number of updraft cores are also investigated with a threshold of 5 m s⁻¹ at each height. The analysis results presented the following findings:

Moved down [4]: Morrison et al.,

Deleted: (e.g.,

Deleted: 2015; Hernández-Deckers and Sherwood, 2016)

Deleted: .

Moved (insertion) [4]

Deleted: and a three-dimensional variational (3DVAR) multi-Doppler radar-based wind retrieval technique (North et al., 2017)

Deleted: were

- As the previous literature has pointed out, the updraft fraction profiles from the simulated wind retrievals suggested that the selected VCP elevation strategy and radar sampling volume resolution affect uncertainties in upper-level (≥ 4.5 km) updraft retrievals, owing to low density and low resolution of radar data attributed to gaps between Plan Position Indicator (PPI) elevation angles and the radar sample volume increasing with distance from the radar. Those uncertainties increase with height above 6 km AGL. In overall experiments using VCPs, stronger updrafts $> 10 \text{ m s}^{-1}$ tend to be underestimated above 4.5 km, while areas of updrafts 5-10 m s^{-1} are overestimated above 6.5 km. Those impact the retrieval of convective mass flux.
- Increasing the maximum elevation angle and the density of the elevation angles of the radar VCP (i.e., 60° over elevation with 1° increment) can effectively improve the updraft retrieval, whereas an addition of data from a Doppler radar cannot significantly improve the updraft retrievals if the added radar VCP has inferior spatial resolutions.
- Shorter duration (2-min or less) radar VCPs are critical to producing high-quality vertical air motion retrievals. The 2-min VCP has small impacts on the snapshot updraft retrievals, but the 5-min VCP induces an important overestimation of areas of updrafts 5–10 m s^{-1} above 6.5 km, underestimation of updrafts $> 10 \text{ m s}^{-1}$ at 4.5 – 8 km, and overestimation of updrafts $\geq 10 \text{ m s}^{-1}$ above 8-9 km.
- The advection correction works to improve the updraft fraction and mean updraft profiles as the profiles become closer to those from the snapshot retrievals and time averaged updraft fields, but it is still challenging to improve stronger updraft retrievals especially for 5-min VCP due to the rapid deformation of the dynamical structures in the simulated mesoscale convective system. The magnitude of improvement by the increase of elevation angles is larger than that by advection correction, even though the VCP needs 2 minutes. However, for the increasing elevations taking 5 minutes, the improvement is less than that from the original VCP completed within 2 minutes.

Deleted: (~

Deleted: using 3 X-SAPRs, and those

Deleted: in this study except the retrieval using the full grid radar data

Deleted: These uncertainties are caused by low density and resolution of radar data attributed to gaps between Plan Position Indicator (PPI) elevation angles and the radar sample volume increasing with distance from the radar.

Deleted: .

Deleted: using multi-Doppler based techniques.

Deleted: and

Deleted: stronger

Deleted: when comparing to the those obtained from the 5-averaged WRF fields and even from the snapshot retrievals. Moreover, the areas

Deleted: stronger

Deleted: (>

Deleted:) are overestimated

Deleted: .5

Deleted: for the 5-min VCP.

Deleted: hard

Deleted: .

Deleted: , which takes

Gridding technique is also an important factor to determine the uncertainties in the wind retrievals. Sophisticated gridding techniques to cover the three-dimensional analysis domain at high spatial resolution, even for higher altitudes, tend to suppress the uncertainty (e.g., Majcen et al., 2008; Collis et

al., 2010; North et al., 2017). Another error source that we did not consider in this study is hydrometeor fall speed estimate, which is generally estimated from radar reflectivity. The sophisticated attenuation correction techniques especially for shorter wavelength radars (e.g., Kim et al, 2008; Gu et al., 2011) and best estimates of hydrometeor fall speeds ([Giangrande, et al., 2013](#)) are required to reduce the wind retrieval uncertainties.

Deleted: Giangrange

In brief, the retrieval of the high-quality vertical velocities in the upper part of convective clouds is very challenging, while the multi-Doppler radar vertical velocity retrievals have been conventionally used to evaluate the CRM simulated dynamical fields. Some of the CRM simulations significantly overestimated compared to multi-Doppler radar vertical velocity retrievals (e.g., Varble et al., 2014; Fan et al., 2017). The present study would suggest that the multi-Doppler radar retrievals for MCSs tend to underestimate the updraft values at middle and upper levels and need to be carefully used considering the limitations of the radar observing system. [The assessment of the multi-Doppler radar retrieval presented in this study could vary for different storm characteristics \(e.g., isolated storm and less wind shear\).](#)

[Although the present study focused on the ARM X-band radar network, the similar dense radar network has been installed in several regions \(e.g., Bousquet et al., 2007; Maesaka, et al. 2011; Helmert et al., 2014\), and field campaigns targeting deep convection \(past, on-going and future\) would be strongly motivated to install multiple Doppler radars to observe vertical air motions in convective clouds. The present analysis can give valuable information to improve the observation strategies and decide optimized scan strategies for the networks.](#) Most of the improvements required in the sampling strategy of the observing system (higher maximum elevation angle, higher density elevation angles and rapid VCP time period) can be accomplished using rapid scan radar systems such as the [Doppler on Wheels mobile radars \(DOWs\)](#), or even phased array radar systems. However, even when such rapid scan radar networks are available, the multi-Doppler retrieval spatial domain will be fairly small compared to the entire radar network coverage. Despite of the limited domain, the observations do cover enough area to track isolated convective updrafts and contain enough samples to derive reliable, low-uncertainty estimates of updraft and downdrafts properties in convective clouds. Spaceborne radar systems with Doppler velocity capability such as the Earth Clouds Aerosols and Radiation Explorer (EarthCARE, Illingworth et al., 2015; Kollias et al., 2018b) or future spaceborne radar concepts (Tanelli et al., 2018) are expected to

Deleted: DOW's

provide additional middle and upper level convective velocity observations especially over the tropical oceans.

Acknowledgements

Portions of this work are funded by the U.S. DOE Office of Science's Biological and Environmental Research Program through the Atmospheric Radiation Measurement (ARM) and Atmospheric System Research (ASR) programs. P. Kollias is also supported by U.S. DOE grant DE- SC0012704. The contribution of A. Shapiro has been supported by NSF grant AGS-1623626. The source code and user manual for the Cloud Resolving Model Radar Simulator (CR-SIM) are available at <https://www.bnl.gov/CMAS/cr-sim.php>.

10 References

Barnes, S. L.: A technique for maximizing details in numerical weather map analysis, *J. Appl. Meteor.*, 3, 396–409, doi: 10.1175/1520-0450(1964)003<0396:ATFMDI>2.0.CO;2, 1964.

[Bell, M. M., Montgomery, M. T., and Emanuel, K. A.: Air–sea enthalpy and momentum exchange at major hurricane wind speeds observed during CBLAST. *J. Atmos. Sci.*, 69, 3197–3222, doi: 10.1175/JAS-D-11-0276, 2012.](#)

Bousquet, O. and Chong, M.: A Multiple-Doppler Synthesis and Continuity Adjustment Technique (MUSCAT) to recover wind components from Doppler radar measurements, *J. Atmos. Oceanic Technol.*, 15, 343–359, doi: 10.1175/1520-0426(1998)015<0343%3AAMDSAC>2.0.CO%3B2, 1998.

20 Bousquet, O., Tabary, P., and Parent du Châtelet, J.: On the value of operationally synthesized multiple-Doppler wind fields, *Geophys. Res. Lett.*, 34, L22813, doi:10.1029/2007GL030464, 2007.

Bousquet, O., Tabary, P., and Parent du Châtelet, J.: Operational multiple-Doppler wind retrieval inferred from long-range radial velocity measurements, *J. Appl. Meteor. Climatol.*, 47, 2929–2945, doi: 10.1175/2008JAMC1878.1, 2008.

- Byers, H. R. and Braham, R. R.: Thunderstorm structure and circulation, *J. Meteor.*, 5, 71–86, 1948, doi: 10.1175/1520-0469(1948)005<0071:TSAC>2.0.CO;2, 1948.
- Caya, A.: Assimilation of radar observations into a cloud-resolving model, Ph.d., McGill University, Montreal, Quebec, 2001.
- 5 Chong, M. and Campos, C.: Extended overdetermined dual-Doppler formalism in synthesizing airborne Doppler radar data, *J. Atmos. Oceanic Technol.* 13, 581-597, doi: 10.1175/1520-0426(1996)013<0581:EODDFI>2.0.CO;2, 1996.
- Chong, M. and Testud, J.: Three-dimensional air circulation in a squall line from airborne dual-beam Doppler radar data: A test of coplane methodology software, *J. Atmos. Oceanic Technol.* 13, 36-53, doi: 10.1175/1520-0426(1996)013<0036%3ATDACIA>2.0.CO%3B2, 1996.
- 10 Clark, T. L., Harris, F. I., and Mohr, C. G.: Errors in wind fields derived from multiple-Doppler radars: Random errors and temporal errors associated with advection and evolution, *J. Appl. Meteor.*, 19, 1273–1284, 1980.
- Collis, C., Protat, A., May, P. T., and Williams, C.: Statistics of storm updraft velocities from TWP-ICE including verification with profiling measurements, *J. Appl. Meteor. Climatol.*, 52, 1909-1922, doi: 10.1175/JAMC-D-12-0230.1, 2013.
- 15 Collis, S., Protat, A., and Chung, K.-S.: The effect of radial velocity gridding artifacts on variationally retrieved vertical velocities. *J. Atmos. Oceanic Technol.*, 27, 1239–1246, 2010.
- Cressman, G. P.: An operational objective analysis system, *Mon. Wea. Rev.*, 87, 367–374, doi: 10.1175/1520-0493(1959)087<0367:AOOAS>2.0.CO;2, 1959.
- 20 Dolan, B. A., and Rutledge, S. A.: An integrated display and analysis methodology for multivariable radar data. *J. Appl. Meteor. Climatol.*, 46, 1196–1213, doi: 10.1175/JAM2524.1, 2007.
- Donner, L. J., Seman, C. J., Hemler, R. S., and Fan, S.: A cumulus parameterization including mass fluxes, convective vertical velocities, and mesoscale effects: Thermodynamic and hydrological aspects in a general circulation model, *J. Climate*, 14, 3444–3463, doi: 10.1175/1520-0442(2001)014<3444:ACPIMF>2.0.CO;2, 2001.
- 25

- Donner, L. J., O'Brien, T. A., Rieger, D., Vogel, B., and Cooke, W. F.: Are atmospheric updrafts a key to unlocking climate forcing and sensitivity?, *Atmos. Chem. Phys.*, 16, 12983-12992, doi:10.5194/acp-16-12983-2016, 2016.
- Fan, J., Han, B., Varble, A., Morrison, H., North, K., Kollias, P., Chen, B., Dong, X., Giangrande, S. E.,
5 Khain, A., Lin, Y., Mansell, E., Milbrandt, J. A., Stenz, R., Thompson, G., and Wang, Y.: Cloud-resolving model intercomparison of an MC3E squall line case: Part I—Convective updrafts, *J. Geophys. Res. Atmos.*, 122, 9351–9378, doi:10.1002/2017JD026622, 2017.
- Fridlind, A. M., Li, X., Wu, D., van Lier-Walqui, M., Ackerman, A. S., Tao, W.-K., McFarquhar, G. M.,
Wu, W., Dong, X., Wang, J., Ryzhkov, A., Zhang, P., Poellot, M. R., Neumann, A., and Tomlinson
10 J. M.: Derivation of aerosol profiles for MC3E convection studies and use in simulations of the 20 May squall line case, *Atmos. Chem. Phys.*, 17, 5947-5972, doi: 10.5194/acp-17-5947-2017, 2017.
- Friedrich, K. and Hagen, M.: Wind synthesis and quality control of multiple-Doppler-derived horizontal wind fields, *J. Appl. Meteor.*, 43, 38-57, doi:10.1175/1520-0450(2004)043<0038:WSAQCO>2.0.CO;2, 2004.
- 15 Gal-Chen, T.: Errors in fixed and moving frame of references: Applications for conventional and Doppler radar analysis, *J. Atmos. Sci.*, 39, 2279–2300, 1982.
- Gao, J., Xue, M., Shapiro, A., and Droegemeier, K. K.: A variational method for the analysis of three-dimensional wind fields from two Doppler radars, *Mon. Wea. Rev.*, 127, 2128–2142, doi: 10.1175/1520-0493(1999)127<2128:AVMFTA>2.0.CO;2, 1999.
- 20 Giangrande, S. E., Collis, S., Straka, J., Protat, A., Williams, C., and Krueger, S.: A summary of convective-core vertical velocity properties using ARM UHF wind profilers in Oklahoma, *J. Appl. Meteor. Climatol.*, 52, 2278-2295, doi: 0.1175/JAMC-D-12-0185.1, 2013.
- Given, T. and Ray, P. S.: Response of a two-dimensional dual-Doppler radar wind synthesis, *J. Atmos. Ocean. Tech.*, 11, 239-255, doi: 10.1175/1520-0426(1994)011<0239:ROATDD>2.0.CO;2, 1994.
- 25 Gu, J.-Y., Ryzhkov, A., Zhang, P., Neilley, P., Knight, M., Wolf, B., and Lee, D.-I.: Polarimetric attenuation correction in heavy rain at C band. *J. Appl. Meteor. Climatol.*, 50, 39-58, doi: 10.1175/2010JAMC2258.1, 2011.

Hartmann, D.L., Hendon, H.H., and Houze Jr., R.A.: Some implications of the mesoscale circulations in cloud clusters for large-scale dynamics and climate, *Journal of the Atmospheric Sciences*, 41, 113-121, doi: 10.1175/1520-0469(1984)041<0113:SIOTMC>2.0.CO;2, 1984.

Helmert, K., and Coauthors: DWDs new radar network and post-processing algorithm chain. *Proc. Eighth European Conf. on Radar in Meteorology and Hydrology (ERAD 2014)*, Garmisch-Partenkirchen, Germany, DWD and DLR, 4.4, 2014. [Available online at http://www.pa.op.dlr.de/erad2014/programme/ExtendedAbstracts/237_Helmert.pdf]

Helmus, J. and Collis, S.: The Python ARM Radar Toolkit (Py-ART), a library for working with weather radar data in the Python programming language, *Journal of Open Research Software*, 4, p.e25, 2016.

10 Heymsfield, G. M., Tian, L., Heymsfield, A. J., Li, L., and Guimond, S.: Characteristics of deep tropical and subtropical convection from nadir-viewing high-altitude airborne Doppler radar, *J. Atmos. Sci.*, 67, 285–308, doi: <https://doi.org/10.1175/2009JAS3132.1>, 2010.

Illingworth, A. I., and Coauthors.: The EarthCARE satellite: The next step forward in global measurements of clouds, aerosols, precipitation, and radiation, *Bull. Amer. Meteor. Soc.*, 96 (8), 15 1311-1332, doi: 10.1175/BAMS-D-12-00227.1, 2015.

Jensen, M. P. and Coauthors: The Midlatitude Continental Convective Clouds Experiment (MC3E), *Bull. Amer. Meteor. Soc.*, 1667-1686, doi: 10.1175/BAMS-D-14-00228.1, 2016.

Jorgensen, D. P. and LeMone, M. A.: Vertically velocity characteristics of oceanic convection, *J. Atmos. Sci.*, 46, 621–640, doi: 10.1175/1520-0469(1989)046<0621:VVCOOC>2.0.CO;2, 1989.

20 Junyent, F., Chandrasekar, V., McLaughlin, D., Insanic, E., and Bharadwaj, N.: The CASA Integrated Project 1 Networked Radar System. *J. Atmos. Oceanic Technol.*, **27**, 61–78, doi: 10.1175/2009JTECHA1296.1, 2010.

Isom, B., and Coauthors: The atmospheric imaging radar: Simultaneous volumetric observations using a phased array weather radar. *J. Atmos. Oceanic Technol.*, **30**, 655–675, doi: 10.1175/JTECH-D-12-00063.1, 2013.

25 Kim, D.-S., Maki, M., Lee, D.-I.: Correction of X-band radar reflectivity and differential reflectivity for rain attenuation using differential phase, *Atmospheric Research*, 90, 1-9, doi: 10.1016/j.atmosres.2008.03.001, 2008.

- Kingsmill, D. E. and Houze, Jr., R. A.: Kinematic characteristics of air flowing into and out of precipitating convection over the west Pacific warm pool: An airborne Doppler radar survey, *Q. J. Roy. Meteorol. Soc.*, 125, 1165–1270, doi: <https://doi.org/10.1002/qj.1999.49712555605>, 1999.
- Kumar, V. V., Jakob, C., Protat, A., Williams, C. R., and May, P. T.: Mass-flux characteristics of tropical cumulus clouds from wind profiler observations at Darwin, Australia, *J. Atmos. Sci.*, 72, 1837–1855, doi: 10.1175/JAS-D-14-0259.1, 2015.
- Kollias, P., McLaughlin, D. J., Frasier, S., Oue, M., Luke, E., and Sneddon, A.: Advances and applications in low-power phased array X-band weather radars. Proc. 2018 IEEE Radar Conference, Oklahoma City, OK, USA, doi: 10.1109/RADAR.2018.8378762, 2018a.
- 10 Kollias, P., A. Battaglia, A. Tatarevic, K. Lamer, F. Tridon and L. Pfitzenmaier: The EarthCARE cloud profiling radar (CPR) Doppler measurements in deep convection: challenges, post-processing and science applications. Proc. SPIE 10776, Remote Sensing of the Atmosphere, Clouds and Precipitation doi:10.1117/12.2324321, 2018b.
- Kurri, N. and Huuskonen, A.: Measurements of the transmission loss of a radome at different rain intensities, *J. Atmos. Oceanic Technol.*, **25**, 1590–1599, doi: 10.1175/2008JTECHA1056.1, 2008.
- 15 LeMone, M. A. and Zipser, E. J.: Cumulonimbus vertical velocity events in GATE. Part I: Diameter, intensity and mass flux, *J. Atmos. Sci.*, 37, 2444–2457, doi: 10.1175/1520-0469(1980)037<2444:CVVEIG>2.0.CO;2 1980.
- Lenschow, D. H.: Estimating updraft velocity from an airplane response, *Mon. Wea. Rev.*, 104, 618–627, doi: 10.1175/1520-0493(1976)104<0618:EUVFAA>2.0.CO;2, 1976.
- 20 Lhermitte, R. and Miller, L.: Doppler Radar Methodology for the Observation of Convective Storms. 14th Conf. on Radar Meteor., Tuscon, AZ, *Amer. Meteor. Soc.*, 133-138, 1970.
- Liu, Y.-C., Fan, J., Zhang, G. J., Xu, K.-M., and Ghan, S. J.: Improving representation of convective transport for scale-aware parameterization: 2. Analysis of cloud-resolving model simulations, *J. Geophys. Res. Atmos.*, 120, 3510–3532, doi:10.1002/2014JD022145, 2015.
- 25 [Maesaka, T., Maki, M., Iwanami, K., Tsuchiya, S., Kieda, K., and Hoshi, A.: Operational rainfall estimation by X-band MP radar network in MLIT, Japan. Proc. 35th Int. Conf. on Radar Meteorology.](#)

- Pittsburgh, PA, Amer. Meteor. Soc., 142, 2011. [[Available online at https://ams.confex.com/ams/35Radar/webprogram/Paper191685.html.](https://ams.confex.com/ams/35Radar/webprogram/Paper191685.html)]
- 5 Majcen, M., P. Markowski, Y. Richardson, D. Dowell, J. Wurman: Multipass objective analyses of Doppler radar data, *J. Atmos. Ocean. Tech.*, 25, 1845 – 1858, doi: 10.1175/2008JTECHA1089.1, 2008.
- Mather, J. H., and Voyles, J. W.: The Arm Climate Research Facility: A review of structure and capabilities, *Bull. Amer. Meteor. Soc.*, 94, 377–392, doi: 10.1175/BAMS-D-11-00218.1, 2013.
- 10 Miller, L. J., and Fredrick, S. M.: Custom Editing and Display of Reduced Information in Cartesian space (CEDRIC) manual. National Center for Atmospheric Research, Mesoscale and Microscale Meteorology Division, Boulder, CO, 130 pp, 1998.
- Morrison, H., Morales, A., and Villanueva-Birriel, C.: Concurrent Sensitivities of an Idealized Deep Convective Storm to Parameterization of Microphysics, Horizontal Grid Resolution, and Environmental Static Stability. *Monthly Weather Review*, 143(6), 2082–2104. <http://doi.org/10.1175/MWR-D-14-00271.1>, 2015.
- 15 Morrison, H., Curry, J., and Khvorostyanov, V.: A new double-moment micro-physics parameterization for application in cloud and climate models. Part I: Description, *J. Atmos. Sci.*, 62, 1665–1677, doi:10.1175/JAS3446.1, 2005.
- North, K. W., Oue, M., Kollias, P., Giangrande, S. E., Collis, S. M., and Potvin, C. K.: Vertical air motion retrievals in deep convective clouds using the ARM scanning radar network in Oklahoma during MC3E, *Atmos. Meas. Tech.* 10, 1 – 14, doi: 10.5194/amt-10-2785-2017, 2017.
- 20 Oue, M., Inagaki, K., Shinoda, T., Ohigashi, T., Kouketsu, T., Kato, M., Tsuboki, K., Uyeda H.: Polarimetric Doppler radar analysis of organization of a stationary rainband with changing orientations in July 2010, *J. Meteorol. Soc. Jpn.*, 22, 457-481, doi: 10.2151/jmsj.2014-503, 2014.
- Park, S-G. and Lee, D-K.: Retrieval of High-Resolution Wind Fields over the Southern Korean Peninsula Using the Doppler Weather Radar Network. *Wea. Forecasting*, 24,87–
- 25 103, <https://doi.org/10.1175/2008WAF2007084.1>, 2009.

- Pazmany, A. L., Mead, J. B., Bluestein, H. B., Snyder, J. C., and Houser, J. B.: A mobile rapid-scanning X-band polarimetric (RaXPoL) Doppler radar system. *J. Atmos. Oceanic Technol.*, **30**, 1398–1413, doi: 10.1175/JTECH-D-12-00166.1, 2013.
- Potvin, C. K., Betten, D., Wicker, L. J., Elmore, K. L., and Biggerstaff, M. I.: 3DVAR versus traditional
5 dual-Doppler wind retrievals of a simulated supercell thunderstorm, *Mon. Wea. Rev.*, **140**, 3487–3494, doi: 10.1175/MWR-D-12-00063.1, 2012a.
- Potvin, C. K., Wicker, L. J., and Shapiro A.: Assessing errors in variational dual-Doppler wind syntheses of supercell thunderstorms observed by storm-scale mobile radars, *J. Atmos. Ocean. Tech.*, **29**, 1009–1025, doi: 10.1175/JTECH-D-11-00177.1, 2012b.
- 10 Protat, A., and Zawadzki, I.: A variational method for real-time retrieval of three-dimensional wind field from multiple-Doppler bistatic radar network data. *J. Atmos. Oceanic Technol.*, **16**, 432–449, doi: 10.1175/1520-0426(1999)016<0432:AVMFRT>2.0.CO;2, 1999.
- Qiu, X., Xu, Q., Qiu, C., Nai, K., and Zhang, P.: Retrieving 3D wind field from phased array radar rapid scans. *Advances in Meteorology*, 2013, 792631, 1-16, doi: 10.1155/2013/792631, 2013.
- 15 Shapiro, A., Willingham, K. M., and Potvin, C. K.: Spatially variable advection correction of radar data. Part I: Theoretical considerations, *J. Atmos. Sci.*, **67**, 3445-3456, doi: 10.1175/2010JAS3465.1, 2010a.
- Shapiro, A., Willingham, K. M., and Potvin, C. K.: Spatially variable advection correction of radar data. Part II: Test Results, *J. Atmos. Sci.*, **67**, 3457-3470, doi: 10.1175/2010JAS3466.1, 2010b.
- 20 Sherwood, S. C., Bony, S., and Dufresne, J.-L.: Spread in model climate sensitivity traced to atmospheric convective mixing. *Nature*, **505**, 37-42. Doi:10.1038/nature12829, 2014.
- Steiner, M.: A new relationship between mean Doppler velocity and differential reflectivity, *J. Atmos. Oceanic Technol.*, **8**, 430–443, 1991.
- Su, J., B. Xiang, B. Wang, and T. Li: Abrupt termination of the 2012 Pacific warming and its implication
25 on ENSO prediction. *Geophys. Res. Lett.*, **41**, 9058-9064. doi:10.1002/2014GL062380, 2014.
- Stonitsch, J.R. and Markowski, P.M.: Unusually Long Duration, Multiple-Doppler Radar Observations of a Front in a Convective Boundary Layer. *Mon. Wea. Rev.*, **135**, 93–117, <https://doi.org/10.1175/MWR3261.1>, 2007.

- Tanelli, S., Haddad, Z. S., Im, E., Durden, S. L., Sy, O. O., Peral, E., Sadowy, G. A., Sanchez-Barbettey, M.: Radar concepts for the next generation of spaceborne observations of cloud and precipitation processes. *IEEE Proceedings of Radar Conference*, Oklahoma City, OK, doi: 10.1109/RADAR.2018.8378741, 2018.
- 5 Tao, W.-K., Wu, D., Lang, S., Chern, J.-D., Peters-Lidard, C., Fridlind, A., and Matsui, T.: High-resolution NU-WRF simulations of a deep convective-precipitation system during MC3E: Further improvements and comparisons between Goddard microphysics schemes and observations, *J. Geophys. Res. Atmos.*, 121, 1278–1305, doi:10.1002/2015JD023986, 2016.
- Tatarevic, A., Kollias, P., Oue, M., Wang, D., and Yu, K.: User's Guide CR-SIM SOFTWARE v 3.1,
10 Brookhaven National Laboratory - Stony Brook University - McGill University Radar Science Group, 2018. [Available at <https://www.bnl.gov/CMAS/cr-sim.php>.]
- Timmermans, R. M. A., Schaap, M., and Builtjes, P.: An Observing System Simulation Experiment (OSSE) for Aerosol Optical Depth from Satellites, *J. Atmos. Ocean. Tech.*, 2673 – 2682, doi: 10.1175/2009JTECHA1263.1, 2009.
- 15 Varble, A., Zipser, E. J., Fridlind, A. M., Zhu, P., Ackerman, A. S., Chaboureau, J.-P., Collis, S., Fan, J., Hill, A., and Shipway, B.: Evaluation of cloud-resolving and limited area model intercomparison simulations using TWP-ICE observations: 1. Deep convective updraft properties, *J. Geophys. Res. Atmos.*, 119, 13,891–13,918, doi:10.1002/2013JD021371, 2014.
- Wakasugi, K., Mizutani, A., Matsuo, M., Fukao, S., and Kato, S. : A direct method for deriving drop-size distribution and vertical air velocities from VHF Doppler radar spectra. *J. Atmos. Oceanic Technol.*, **3**, 623–629, doi: 10.1175/1520-0426(1986)003<0623:ADMFDD>2.0.CO;2, 1986.
- Williams, C. R.: Vertical Air Motion Retrieved from Dual-Frequency Profiler Observations. *J. Atmos. Oceanic Technol.*, **29**, 1471–1480, <https://doi.org/10.1175/JTECH-D-11-00176.1>, 2012.
- Wu, J., Del Genio, A. D., Yao, M., and Wolf, A. B.: WRF and GISS SCM simulations of convective
25 updraft properties during TWP-ICE, *J. Geophys. Res.*, 114 (D4), D04206, doi: 10.1029/2008JD010851, 2009.

Wu, W. and McFarquhar, G. M.: On the impacts of different definitions of maximum dimension for nonspherical particles recorded by 2D imaging probes, *J. Atmos. Ocean. Tech.*, 33, 1057-1072, doi: 10.1175/JTECH-D-15-0177.1, 2016.

5 Wurman, J., The DOW mobile multiple-Doppler network. Preprints, 30th Int. Conf. on Radar Meteorology, Munich, Germany, Amer. Meteor. Soc., 95–97, 2001.

Tables and figures

Table 1: Simulated radar configurations and measurement strategy.

	X-SAPR	C-SAPR
Radar frequency (GHz)	9.5	5.5
Beamwidth (degrees)	1.1	1.0
Number of elevation angles	21	17
Elevation angles (degrees)	0.5, 1.5, 2.5, 3.5, 4.5, 5.5, 6.5, 7.5, 8.5, 9.5, 10.5, 11.5, 12.5, 14.0, 17.0, 20.0, 25.0, 30.0, 35.0, 40.0, 45.0	0.8, 1.2, 1.9, 2.6, 3.5, 4.4, 5.3, 6.4, 7.8, 9.6, 11.7, 14.3, 17.5, 21.4, 26.1, 33.0, 42.0
Azimuth spacing (degrees)	1.1	1.0
Maximum observation range (km)	40	120
Range gate spacing (m)	60	120
Radar location	X-SAPRs (I4, I5, and I6) of Fig. 1	C-SAPR I7 of Fig.1
Antenna rotation rate* ($^{\circ} \text{ s}^{-1}$)	28	18

5 * Antenna rotation rates used during the MC3E are presented and not used in this study.

Table 2: Overview and short description of the different sensitivity simulations.

Simulation	Name	Specification
Control	3FullGrid	i) All elevation angles from 3 X-SAPRs at each gridbox of the original WRF snapshot grid at 12:18:00 UTC (no interpolation according to the radar beamwidth is considered)
Radar VCP	3XR	i) 3 X-SAPRs with 21 elevation angles ranging from 0.5 to 45 degrees over elevation angle
	3LRs	ii) 3 X-SAPRs with 60 elevation angles of 60 ranging from 0.5 to 59.5 degrees with equal increment of 1 degree
	4SR	iii) 4 radars including 3 X-SAPRs and the C-SAPR
Time period	Snap	i) Snapshot at 12:18:00
	2min	ii) 2 minutes (6 snapshots)
	5min	iii) 5 minutes (15 snapshots)
Advection correction	(No name)	i) No advection correction
	adv	ii) Advection correction proposed by Shapiro et al. (2010a) for time settings ii) and iii)

Table 3: Root mean square error (RMSE) of UF_5 , UF_{10} , MF_5 , MF_{10} , \bar{w}_5 , and \bar{w}_{10} profiles above 2 km AGL for all experiments.

	UF_5	UF_{10}	MF_5 [$kg\ m^{-2}\ s^{-1}$]	MF_{10} [$kg\ m^{-2}\ s^{-1}$]	\bar{w}_5 [$m\ s^{-1}$]	\bar{w}_{10} [$m\ s^{-1}$]
3FullGrid	0.34×10^{-2}	0.18×10^{-2}	0.23×10^{-1}	0.18×10^{-1}	0.15	1.93
3XRSnap	3.06×10^{-2}	0.68×10^{-2}	0.89×10^{-1}	0.60×10^{-1}	1.18	0.65
3XR2min	3.45×10^{-2}	0.63×10^{-2}	1.02×10^{-1}	0.52×10^{-1}	1.10	0.53
3XR5min	3.26×10^{-2}	1.03×10^{-2}	1.08×10^{-1}	0.95×10^{-1}	1.48	1.01
3LRSnap	1.99×10^{-2}	0.42×10^{-2}	0.68×10^{-1}	0.37×10^{-1}	0.87	0.50
3LR2min	2.44×10^{-2}	0.49×10^{-2}	0.85×10^{-1}	0.41×10^{-1}	0.91	0.52
3LR5min	3.94×10^{-2}	0.92×10^{-2}	1.37×10^{-1}	0.75×10^{-1}	1.23	0.70
4SRSnap	3.57×10^{-2}	0.64×10^{-2}	1.04×10^{-1}	0.56×10^{-1}	1.12	0.67
4SR2min	3.43×10^{-2}	0.66×10^{-2}	1.04×10^{-1}	0.57×10^{-1}	1.06	0.56
4SR5min	5.79×10^{-2}	1.10×10^{-2}	1.91×10^{-1}	0.83×10^{-1}	1.33	0.81
3XR2minadv	2.90×10^{-2}	0.75×10^{-2}	0.96×10^{-1}	0.65×10^{-1}	1.11	0.61
3XR5minadv	3.38×10^{-2}	0.96×10^{-2}	1.10×10^{-1}	0.88×10^{-1}	1.28	0.89
3LR2minadv	1.39×10^{-2}	0.71×10^{-2}	0.64×10^{-1}	0.64×10^{-1}	0.90	0.66
3LR5minadv	1.55×10^{-2}	1.15×10^{-2}	0.85×10^{-1}	1.02×10^{-1}	1.40	0.85
3XRSnap (limited area)	5.09×10^{-2}	1.29×10^{-2}	1.53×10^{-1}	1.08×10^{-1}	1.06	2.86
3XR2min (limited area)	4.73×10^{-2}	1.48×10^{-2}	1.69×10^{-1}	1.20×10^{-1}	0.86	0.96
3LRSnap (limited area)	2.24×10^{-2}	0.89×10^{-2}	0.79×10^{-1}	0.83×10^{-1}	0.71	2.87
3LR2min (limited area)	2.19×10^{-2}	1.28×10^{-2}	0.84×10^{-1}	1.19×10^{-1}	0.81	0.88
4SRSnap (limited area)	5.83×10^{-2}	1.11×10^{-2}	1.74×10^{-1}	0.94×10^{-1}	0.93	2.84

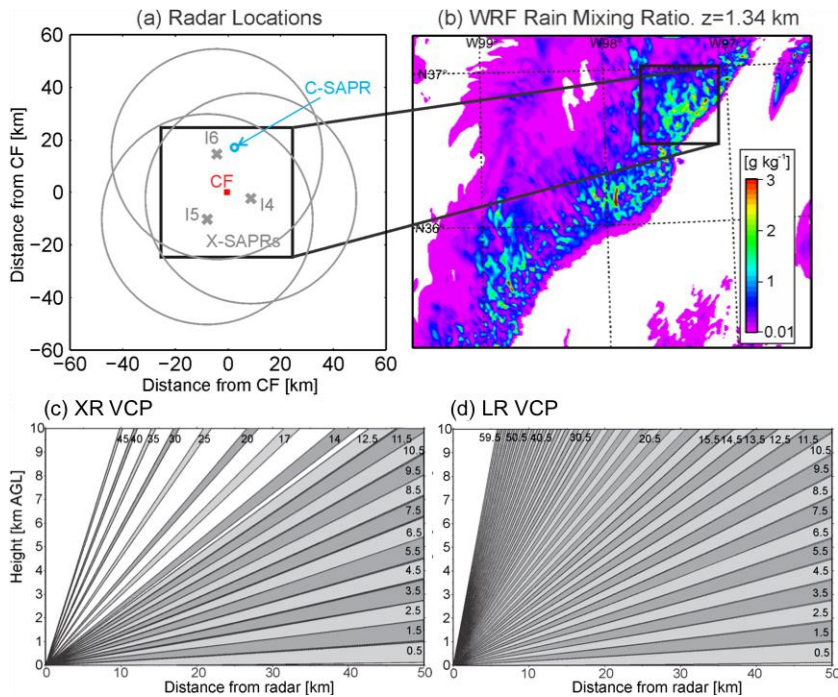


Figure 1: (a) Locations of radars and the Department of Energy Atmospheric Radiation Measurements (ARM) Central Facility. Large gray circles represent maximum range of each X-band Scanning ARM Precipitation Radar (X-SAPR). (b) Rain water mixing ratios at 1.3 km altitude from the WRF simulation of a mesoscale convective system at 12:18:00 UTC on 20 May 2011. Black boxes represent the domain used for wind retrievals. (c and d) Elevation coverage for X-SAPR general VCP (XR) and high-density elevation volume coverage pattern (VCP) (LR), respectively.

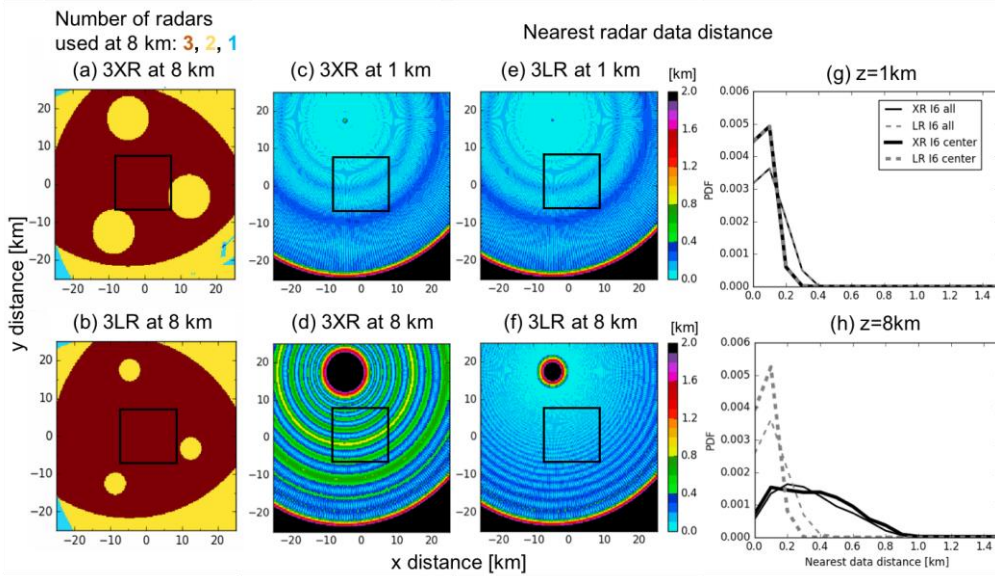
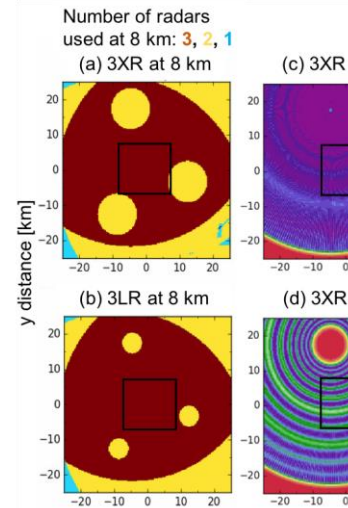


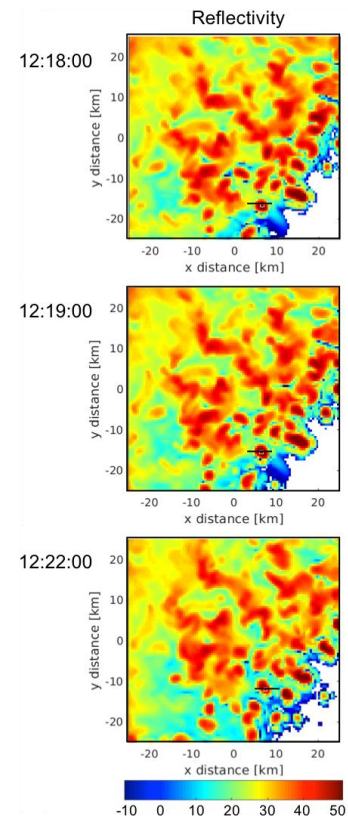
Figure 2: (a and b) Number of radars used for retrievals at each grid box at 8 km above ground level (AGL) for 3XR VCP (a) and 3LR VCP (b), (c-f) distance of nearest radar data point at each grid box at 1 km (c and e) and 8 km (d and f) for the radar location of I6 with XR VCP (c and d) and LR VCP (e and f), and (g and h) histograms of the distance of nearest radar data point at 1 km (g) and 8 km (h) AGL normalized by the total number of data samples and the nearest distance bin size (0.1 km). In g and h, black solid lines represent the radar location of I6 with XR VCP, gray dashed lines represent the radar location of I6 with LR VCP, thin lines represent the entire horizontal domain, and thick lines represent a box area shown in (a-f).

5

10



Deleted:



Deleted:

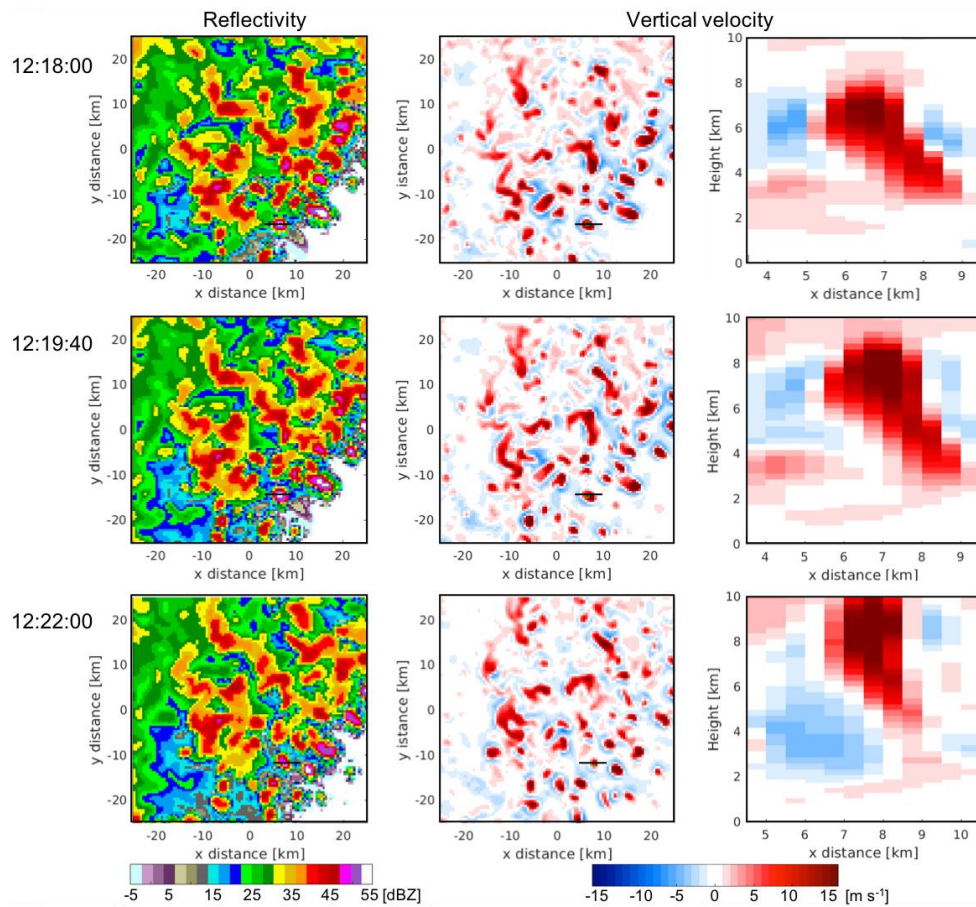


Figure 3: (Left column) Horizontal distributions of X-band Z at 7 km AGL from CR-SIM, (middle column) horizontal distributions of the WRF simulated vertical velocity at 7 km AGL, and (right column) vertical distributions of WRF-simulated vertical velocity along a line in the horizontal plots. Each row from top to bottom represents simulation time of 12:18:00, 12:19:40, and 12:22:00 UTC, respectively.

Deleted: radar reflectivity

Deleted: 00

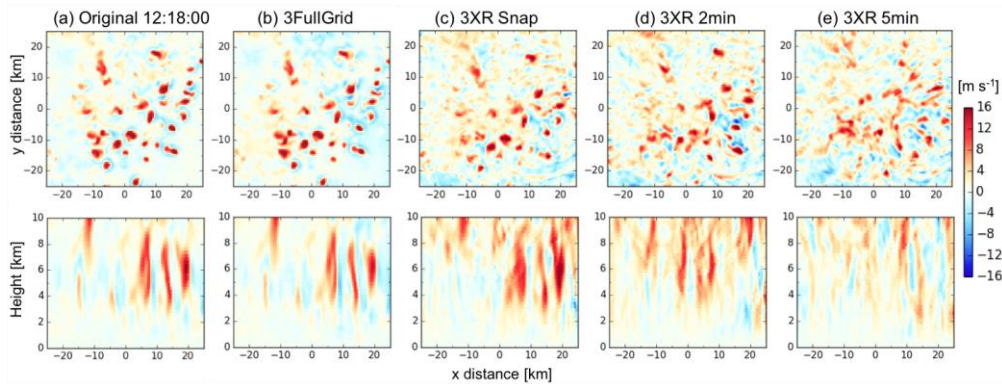


Figure 4: (Top row) Horizontal distributions at 7 km AGL and (bottom row) vertical cross sections at $y = 0$ km of vertical velocity. Each column represents (a) the original WRF vertical velocity field and retrieved vertical velocity from (b) the 3FullGrid, (c) 3XRSnap, (d) 3XR2min, and (e) 3XR5min retrieval simulations.

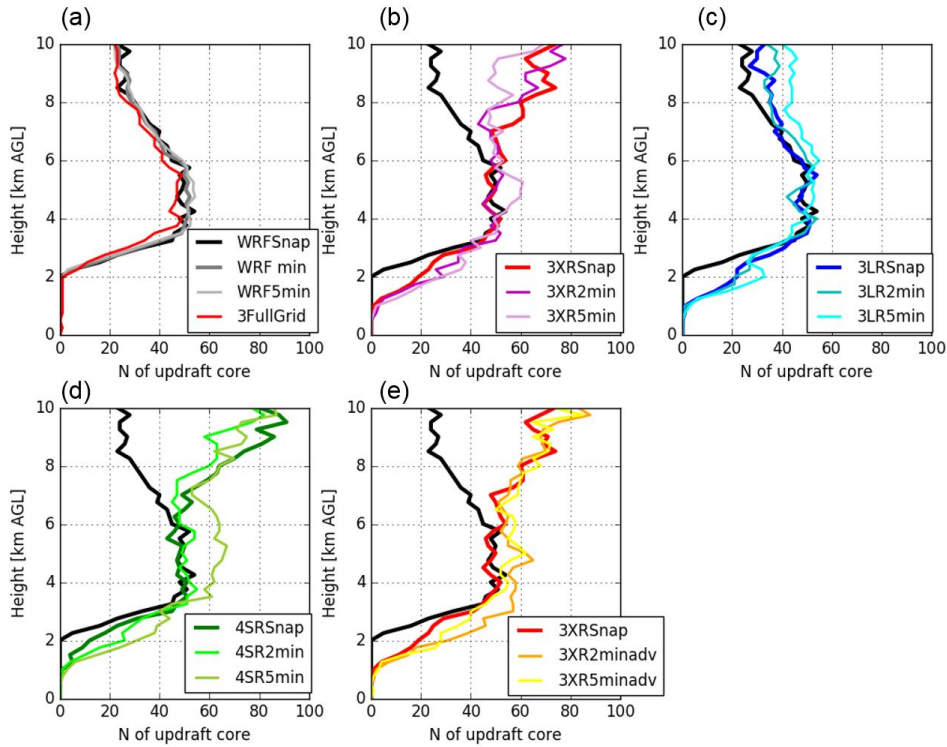


Figure 5: Vertical profiles of the number of coherent updrafts with vertical velocity $> 5 \text{ m s}^{-1}$. Colour represents different retrieval simulations as displayed in each panel. Dark gray line in (a) represents time average of the WRF output over 2 minutes from 12:18:00 to 12:19:40 UTC, and light gray in (a) represents time average of the WRF output over 5 min from 12:18:00 to 12:22:40 UTC. Each panel displays a profile from the WRF snapshot at 12:18:00 UTC by a black solid line.

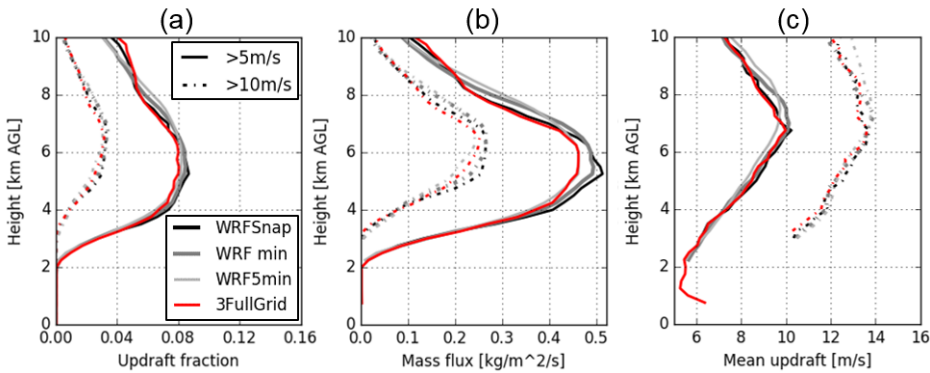
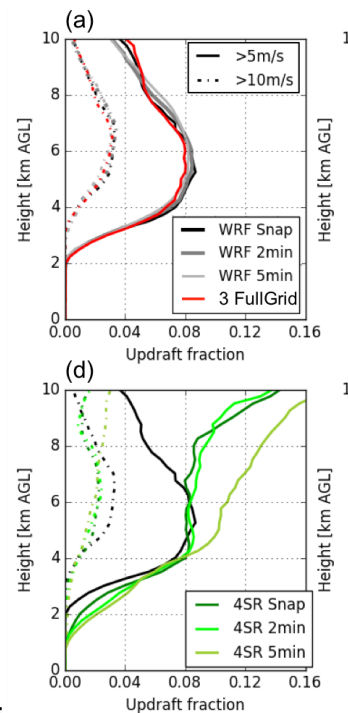


Figure 6: Vertical profiles of (a) updraft fraction, (b) mass flux, and (c) mean updraft velocity, with different thresholds of 5 m s^{-1} (solid lines) and 10 m s^{-1} (dashed lines) for the entire retrieval domain. Black lines represents the WRF snapshot at 12:18:00 UTC, dark gray lines represent time average of the WRF output over 2 minutes from 12:18:00 to 12:19:40 UTC, and light gray lines represent time average of the WRF output over 5 min from 12:18:00 to 12:22:40 UTC. Red lines represents the 3FullGrid retrieval simulations.



Deleted:

Deleted: fractions

Deleted: (a – e) and a center region shown as a box in Fig. (f). Color

Deleted: different

Deleted: as displayed in each panel.

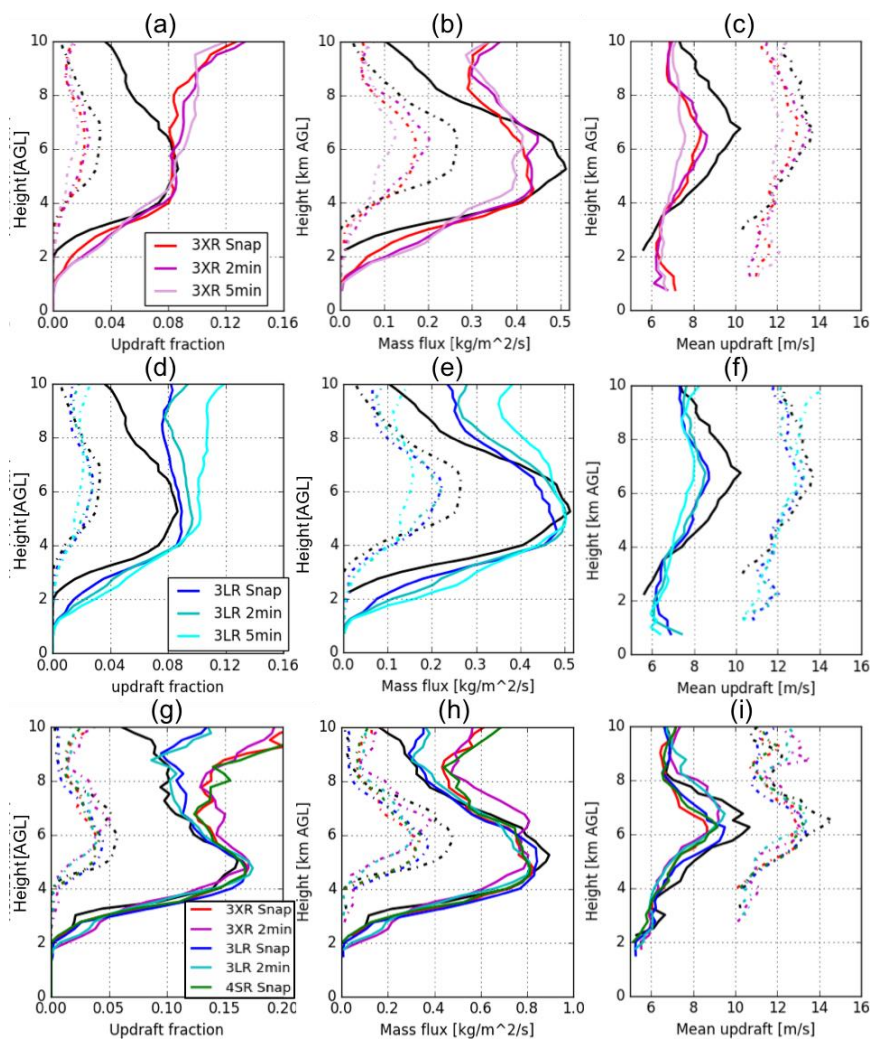
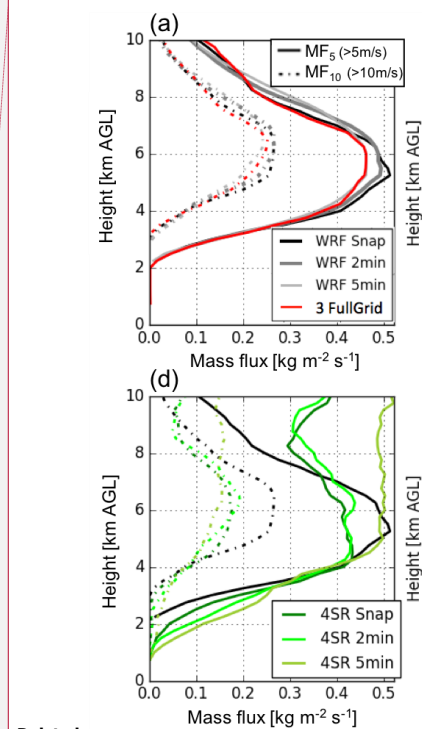


Figure 7: Vertical profiles of (left column) updraft fraction, (middle column) mass flux, and (right column) mean updraft velocity, with different thresholds of 5 m s^{-1} (solid lines) and 10 m s^{-1} (dashed lines) for the entire retrieval domain (a – f) and a center region shown as a box in Fig. 2 (g – h).



Deleted:

Deleted: convective

Deleted: updraft

Deleted: -e

Deleted: f

Color represents different retrieval simulations as displayed in panels in the left column. Each panel displays profiles from the WRF snapshot at 12:18:00 UTC by black lines.

Deleted: each

Deleted: .

5

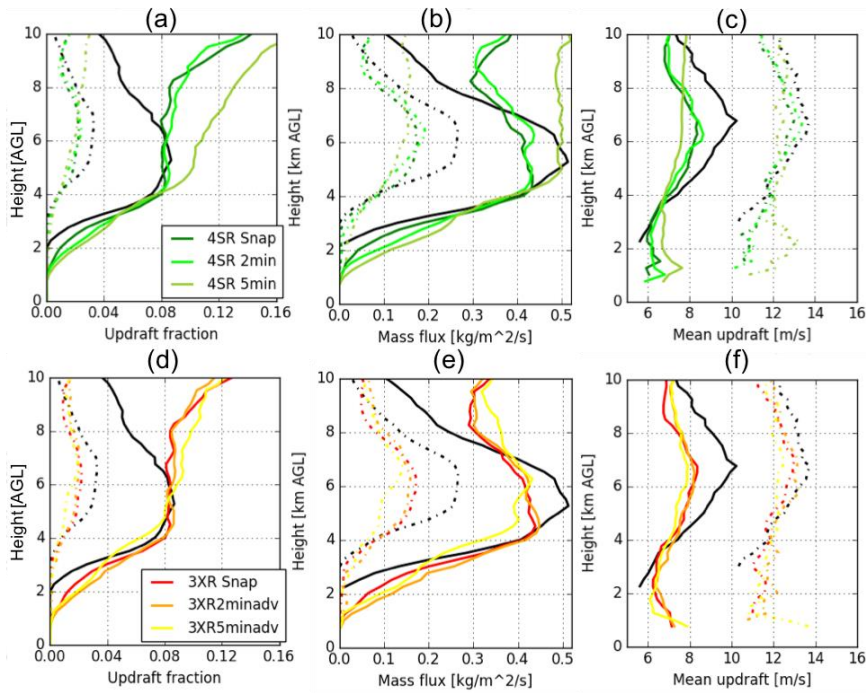
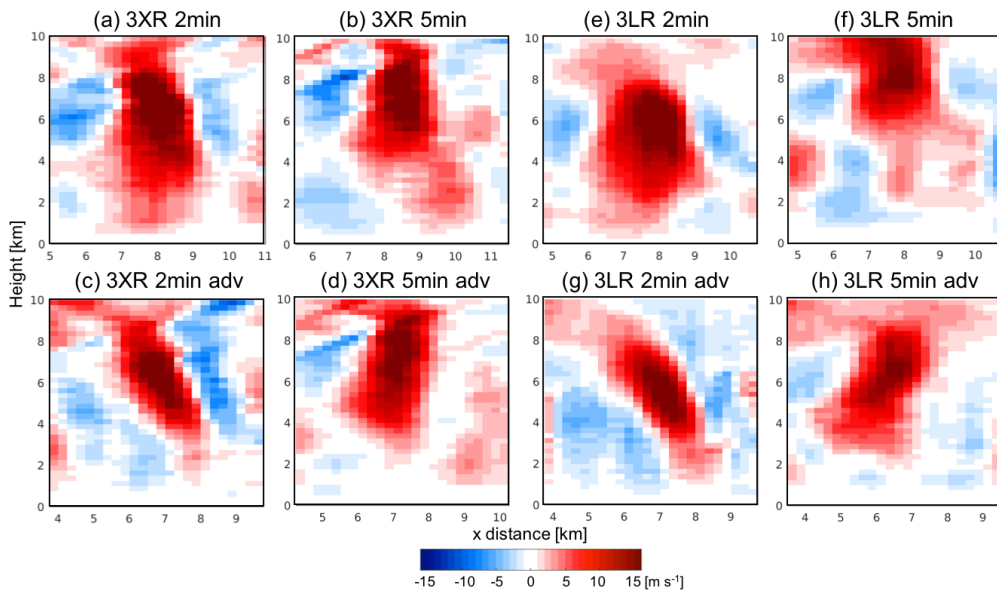


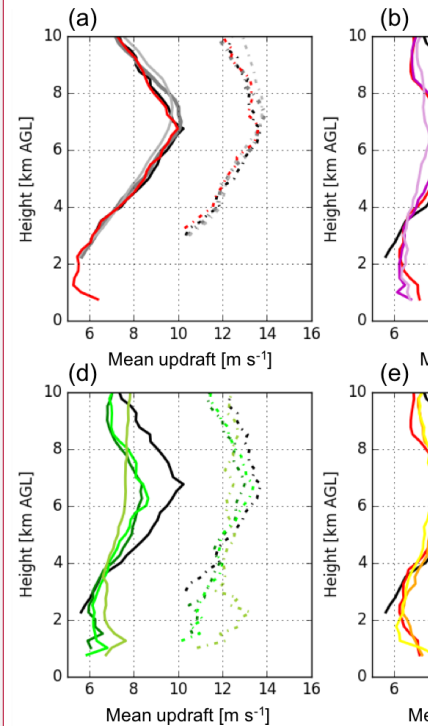
Figure 8: Vertical profiles of (left column) updraft fraction, (middle column) mass flux, and (right column) mean updraft velocity, with different thresholds of 5 m s^{-1} (solid lines) and 10 m s^{-1} (dashed lines) for the entire retrieval domain (a – f). Color represents different retrieval simulations as displayed in panels in the left column. Each panel displays profiles from the WRF snapshot at 12:18:00 UTC by black lines.

10



5 **Figure 9:** Vertical cross sections of vertical velocity for an updraft core from 3XR (a-d) and 3LR (e-h) wind retrieval simulations with 2-min and 5-min VCPs. Top row and bottom row display non-advection correction and advection-corrected retrievals, respectively. A selected updraft core is the same as shown in Fig. 3.

Deleted: ¶



¶ **Figure 8:** Same as Figure 7, but for mean updraft. Color representation is same as Figure 7. ¶